Taylor & Francis
Taylor & Francis Group

Journal of Biomolecular Structure and Dynamics

ISSN: (Print) (Online) Journal homepage: https://www.tandfonline.com/loi/tbsd20

Synthesis and spectroscopic characterizations of hexakis[(1-(4'-oxyphenyl)-3-(substituted-phenyl)prop-2-en-1-one)]cyclotriphosphazenes: their *in vitro* cytotoxic activity, theoretical analysis and molecular docking studies

Hacer Doğan, Mehmet Refik Bahar, Eray Çalışkan, Suat Tekin, Harun Uslu, Feride Akman, Kenan Koran, Süleyman Sandal & Ahmet Orhan Görgülü

To cite this article: Hacer Doğan, Mehmet Refik Bahar, Eray Çalışkan, Suat Tekin, Harun Uslu, Feride Akman, Kenan Koran, Süleyman Sandal & Ahmet Orhan Görgülü (2022) Synthesis and spectroscopic characterizations of hexakis[(1-(4'-oxyphenyl)-3-(substituted-phenyl)prop-2-en-1-one)]cyclotriphosphazenes: their *in vitro* cytotoxic activity, theoretical analysis and molecular docking studies, Journal of Biomolecular Structure and Dynamics, 40:7, 3258-3272, DOI: 10.1080/07391102.2020.1846621

To link to this article: https://doi.org/10.1080/07391102.2020.1846621

Published online: 19 Nov 2020.

JOURNAL OF BIOMOLECULAR STRUCTURE AND DYNAMICS
2022, VOL. 40, NO. 7, 3258–3272
https://doi.org/10.1080/07391102.2020.1846621

Synthesis and spectroscopic characterizations of hexakis[(1-(4′-oxyphenyl)-3-(substituted-phenyl)prop-2-en-1-one)]cyclotriphosphazenes: their *in vitro* cytotoxic activity, theoretical analysis and molecular docking studies

Hacer Doğan[a], Mehmet Refik Bahar[b], Eray Çalışkan[c], Suat Tekin[b], Harun Uslu[d], Feride Akman[e], Kenan Koran[f], Süleyman Sandal[b] and Ahmet Orhan Görgülü[a]

[a]Chemistry Department, Science Faculty, Firat University, Elazığ, Turkey; [b]Physiology Department, Faculty of Medicine, Inonu University, Malatya, Turkey; [c]Department of Chemistry, Faculty of Science, Bingol University, Bingol, Turkey; [d]Department of Anesthesiology, Vocational School of Health Services, Firat University, Elazığ, Turkey; [e]Vocational School of Technical Sciences, Bingol University, Bingol, Turkey; [f]Department of Food Processing, Karakoçan Voc. School, Firat University, Elazığ, Turkey

Communicated by Ramaswamy H. Sarma

ABSTRACT

The hexachlorocyclotriphosphaze compound **($N_3P_3Cl_6$, HCCP)** was reacted with excess (E)-(1-(4′-oxyphenyl)-3-(substituted-phenyl)prop-2-en-1-ones **(2-11)** to produce hexakis[(1-(4-oxyphenyl)-3-(substituted-phenyl)prop-2-en-1-one)]cyclotriphosphazenes **(CP 2-11)**. The structures of products **(CP 2-11)** were confirmed using elemental analysis, FT-IR, MS spectral analysis as well as ^{31}P, ^{1}H and ^{13}C-APT NMR techniques and their thermal properties determined by TGA and DSC techniques. The HOMO-LUMO energy gap and chemical reactivity identifiers were calculated and HOMO and LUMO images were viewed. According to the calculations, all the chemical potential values of **CP 2-11** are negative and it shown that the molecules are stable. The *in vitro* cytotoxic of **CP 2-11** investigated and their activity potentials were evaluated by molecular docking studies with Autodock Vina softwares. **CP 2-11** compounds were found to demonstrate cytotoxic activity against human cancer cell lines (A2780, LNCaP and PC-3). The **CP 2-11** compounds reduced the cell viability against all cancer cell lines in the range 36%–90% especially. The results showed that these compounds are powerful candidate molecules for pharmaceutical applications.

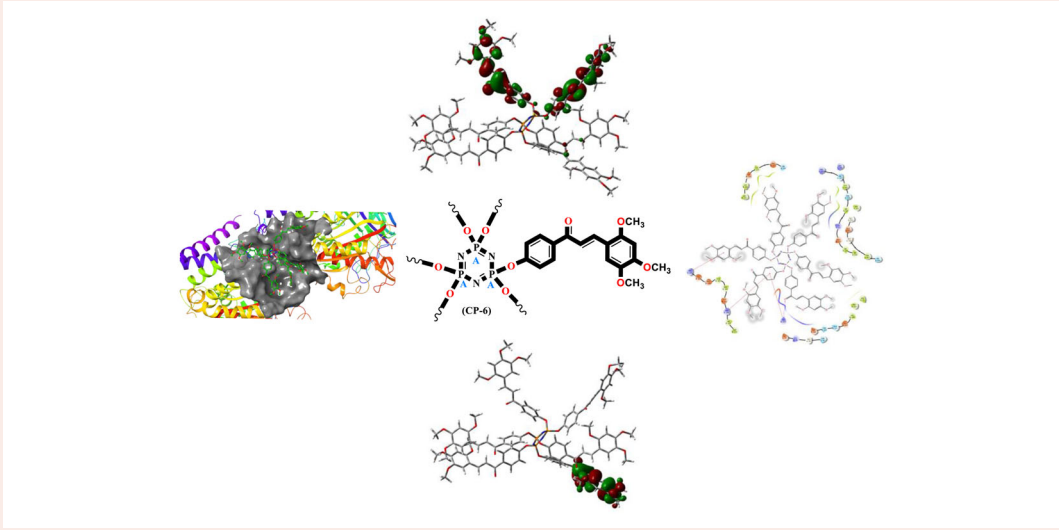

Synthesis, spectroscopic and thermal properties, *in vitro* cytotoxic properties, theoretical analysis and molecular docking studies of hexa substituted cyclotriphosphazenes **CP 2-11** were investigated.

ARTICLE HISTORY
Received 31 May 2020
Accepted 1 November 2020

KEYWORDS
MTT assay; spiro-phosphazene; cytotoxicity; molecular docking; structural characterizations

1. Introduction

Phosphazenes, which is an important class in inorganic compounds, are synthesized by the reaction of phosphorus compounds and nucleophiles containing nitrogen atoms. Phosphazene compounds containing phosphorus–nitrogen bonds in their structure are bounded by two organic or inorganic side groups (R) in each phosphorus atom in repeated –P = N– units. Their general structure can be straight chain,

CONTACT Kenan Koran kenan.koran@gmail.com Department of Food Processing, Karakoçan Voc. School, Firat University, Elazığ 23600, Turkey

cyclic or polymeric (Allcock, 1972; Gleria & De Jaeger, 2004). Reactive –Cl atoms in their structure provide many important reactions such as alcoholism, phenolysis, hydrolysis, aminolysis and Friedel-Crafts (Akbaş et al., 2013; Çoşut et al., 2009; Kuan & Lin, 2004; McBee et al., 1965; Siwy et al., 2006). Due to the chlorine atoms in its structure, substitution reactions with -di, -tri, tetra, penta or hexa function can be performed with aliphatic or aromatic nucleophiles (Chen et al., 2019; İbişoğlu et al., 2020; Lee et al., 2020). The cyclic phosphosphazene was chosen as the main skeleton because of its characteristics such as the easy functioning of the cyclic phosphazene compounds, the stability of the substituted phosphazenes, the possibility of different biological or physical properties depending on the characteristics of the substituted side groups, and the possibility of multiple functional groups to coexist (Andrianov, 2008; Gleria & De Jaeger, 2004).

Substitution reactions, one of the most important reactions in phosphazene chemistry, take place with nucleophiles such as alcohol, phenol and diol. The most important reason why these reactions take place in numerous studies is that the by-product formation is minimal and the products formed are stable, which allows the products to be purified and characterized easily. It is another factor in the study that the aryloxy substituted phosphazene compounds have very high thermal and hydrolytic stability (Allcock, 1972; Koran & Görgülü, 2018; Shaw, 1986). Such properties have made these structures important compounds that can be used both in obtaining high temperature resistant materials and in synthesizing new polymers. Halocyclotriphosphazene compounds can be easily obtained in a suitable organic solvent medium using sodium or potassium salts of alcohol or phenols or a base such as triethylamine, potassium or sodium carbonate (Carriedo et al., 1996; Görgülü et al., 2015; Koran et al., 2016). Depending on the properties of the substituted groups on the cyclotriphosphazene compound, these compounds can display many different properties, including nonlinear optics, solar cell and photodiode, electrical properties, chemical sensor, tribological behavior and OFET application, antimicrobial and cytotoxic activities (Alidağı et al., 2013; Asmafiliz et al., 2019; Bolink et al., 2008; Destegül et al., 2019; Elgazzar et al., 2017; Fei et al., 2008, 2011; Hadji & Rahmouni, 2016; Koran, 2019; Özcan et al., 2019; Tanrıverdi Eçik et al., 2019).

The articles on the synthesis of cyclic phosphazenes and the investigation of their various biological and physical properties have been reported in the literature (Bobrov et al., 2020; Dagdag et al., 2019; Januszewski et al., 2018; Jiang et al., 2015; Nikovskii et al., 2018; Tümer et al., 2018; Wang et al., 2018; Yang et al., 2019). There are, however, no studies about synthesis, *in vitro* cytotoxic activity, theoretical analysis and molecular docking studies of hexa substituted cyclotriphosphazene compounds **CP 2-11**.

The aim of this study is to prepare hexa substituents of cyclotriphosphazenes, which constitute an important class of thermally stable inorganic heterocyclic compounds, and to investigate *in vitro* cytotoxicity properties, theoretical analysis and molecular docking studies. Firstly, compounds **2-11** were synthesized according to Claisen-Schmidt condensation by the method in the literature (Bist et al., 2017; Brian et al., 1989; Chaudhary et al., 2020, 2020; Chimenti et al., 2004; Ingle & Upadhyay, 2005; Jeyasheela & Subramanian, 2019; Mirzaei et al., 2020; Satyanarayana et al., 2004; Shenvi et al., 2013; Xie et al., 2011). In the second stage, hexa substituted cyclophosphazene compounds **CP 2-11** were obtained by reaction of the compounds **2-11** obtained in the previous step with the compound of hexachlorocyclotriphosphazene (**HCCP**). The structures of these pure compounds were characterized using ^{31}P, ^{1}H-NMR, ^{13}C-APT NMR, FT-IR and MALTI-TOF MS spectroscopic methods. In addition, thermal stability of the compounds was determined by taking DSC and TGA thermograms. The HOMO-LUMO energy gap and chemical reactivity identifiers were calculated using the Gaussian 09W package in DFT (B3LYP) methods set on the basis of 6-31G (d, p), and HOMO and LUMO images were viewed using GaussView 5.0. In the last step, hexa substituted cyclotriphosphazenes **CP 2-11** at different concentrations (1, 5, 25 and 50 μM) are employed against human ovarian (A2780) and human prostate (PC-3 and LNCaP) cancer cell lines to investigate % cell viability and *in vitro* cytotoxicity activities using the MTT assay method. LogIC50/IC50 values of the compounds were calculated. **CP 2-11** compounds were found to demonstrate cytotoxic activity against human cancer cell lines (A2780, LNCaP and PC-3). The results showed that these compounds are powerful candidate molecules for pharmaceutical applications. Disruption of the microtubules can lead to apoptosis induction as it has vital importance to the continuation of the cell cycle (Carlson, 2008). Therefore, the literature emphasizes that tubulin inhibitors can be used as effective anticancer drugs (Prota et al., 2014; Sengupta & Thomas, 2006). Binding sites for colchicine is well determined in the tubule (Fleming, 2010). Potential tubulin inhibition effects with synthesized molecules were determined by Tubulin–Colchicine complex. The interactions of compounds with the Tubulin–Colchicine complex were put forth via molecular docking studies.

2. Experimental section

2.1. Materials and measurements

All the chemicals were bought from Sigma-Aldrich and Merck. ^{1}H and ^{13}C-APT NMR spectra were recorded via Bruker DPX-400 MHz spectrometer and Perkin Elmer FT-IR spectrometer was used for Infrared analysis. Microanalysis was acquired by a LECO 932 CHNS-O apparatus. Mass spectra were obtained by a Bruker microflex LT MALDI-TOF MS spectrometer. The thermal behavior of hexa substituted cyclotriphosphazenes was investigated by differential scanning calorimetry (DSC, 20 °C/min) and thermogravimetric analysis (TGA, 10 °C/min) using a SHIMADZU. Human prostate (PC-3 and LNCaP) and ovarian cancer cell lines required for cell culture studies were purchased from ATCC (American Type Culture Collection). Penicillin, trypsin, streptomycin, newborn calf serum and Dulbecco's modified Eagle's medium (DMEM) were purchased from Hyclone (Waltham, MA, USA). Panasonic was used as a CO_2 incubator, Nuve MN-120 as a

biological safety cabinet, BioTEK spectrophotometer as a microplate reader, Reverse Microscope SOIF-XDS for cell maintenance and control, and Nuve was preferred for sterilization.

2.2. Synthesis and characterization

Starting compounds **2-11** were synthesized according to the procedure reported in the literature. A similar method was used in the synthesis of **CP 2-11**. The detailed procedure of the reaction is given only in the synthesis of the compound **CP-2**.

2.2.1. Synthesis of hexakis[(1-(4′-oxyphenyl)-3-(3-methoxyphenyl)prop-2-en-1-one)]cyclotriphosphazene (CP-2)

After the argon and airless medium reaction apparatus was prepared, 0.58 mmol (0.2 g) **HCCP** was added to the three necked reaction flask containing 40 mL of dry acetone at 0 °C. 4.03 mmol (0.56 g) of anhydrous K_2CO_3 was added to this mixture and the reaction was stirred for 30 min. Finally, the solution of **2** (3.49 mmol, 0.89 g) in acetone was added dropwise to the mixture. The reaction was then stirred for about 1 h. Then it was mixed with magnetic stirrer by heating at the boiling point of acetone. The reaction was stopped by following thin layer chromatography. Reaction time is about 12 h. After the reaction was stopped, the solid in the reaction medium was filtered off. After some of the acetone was evaporated, it was precipitated by adding 3% to 250 mL NaOH solution. The precipitated solid was filtered off and washed with plenty of water until pH 7. Finally, it was washed with ethyl alcohol and dried. The dried solid was again dissolved in chloroform and precipitated in *n*-hexane. It was obtained as pure in 85% yield. White solid; m.p. 125–126 °C. MALDI-MS: $N_3P_3O_{18}C_{96}H_{78}$ *m/z* calc. 1654.60; found: 1655.10 $[M+H]^+$. Microanalysis: Found: C 70.02, H 4.79%. requires C 69.69, H 4.75%. FT-IR (KBr) ν_{max} (cm^{-1}): 3001 and 3065 ν_{Ar-CH}, 2837 and 2961 $\nu_{Aliphatic-CH}$, 1658 $\nu_{C=O}$, 1501, 1578 and 1597 $\nu_{C=C}$, 1158 and 1178 $\nu_{P=N}$, 949 ν_{P-O-Ph}. ^{31}P-NMR (DMSO-d_6, ppm) $\delta = 8.10$ (3P, s, PA, A3). ^{1}H NMR (DMSO-d_6, ppm) $\delta = 3.81$ (18H, s, H^{16} ($-OCH_3$)), 7.0–7.03 (6H, d, Ar–H^{13}), 7.16–7.18 (12H, d, $J = 8.4$ Hz, Ar–$H^{3,5}$), 7.33–7.38 (18H, m, Ar–$H^{11,14,15}$), 7.60–7.64 6, d, $J = 15.6$ Hz, H^8 (–CH=)), 7.79–7.83 (6H, d, $J = 15.6$ Hz, H^9 (=CH–)) and 8.06–8.08 (12H, d, $J = 8.4$ Hz, Ar–$H^{2,6}$).^{13}C-APT NMR (DMSO-d_6, ppm) $\delta = 135.41$ Ar–C^1, 131.15 Ar–$C^{2,6}$, 121.19 Ar–$C^{3,5}$, 153.40 Ar–C^4, 188.18 C^7 (–C = O), 122.16 C^8 (–CH=), 144.79 C^9 (=CH–), 136.35 Ar–C^{10}, 121.19 Ar–C^{11}, 160.04 Ar–C^{12}, 113.95 Ar–C^{13}, 130.31 Ar–C^{14}, 122.08 Ar–C^{15} and 55.71 C^{16} ($-OCH_3$).

2.2.2. Synthesis of hexakis[(1-(4′-oxyphenyl)-3-(2,4-dimethoxyphenyl)prop-2-en-1-one)]cyclotriphosphazene (CP-3)

The procedure is similar to that of **CP-2**, using **HCCP** (0.2 g, 0.58 mmol), **3** (1 g, 3.49 mmol) and K_2CO_3 (0.56 g, 4.03 mmol). Yield: 77%; white solid. m.p. 135–136 °C. MALDI-MS: $N_3P_3O_{24}C_{102}H_{90}$ *m/z* calc. 1834.76; found: 1834.286.

Microanalysis: Found: C 66.79, H 4.96%. requires C 66.77, H 4.94%. FT-IR (KBr) ν_{max} (cm^{-1}): 3008 and 3058 ν_{Ar-CH}, 2837 and 2941 $\nu_{Aliphatic-CH}$, 1655 $\nu_{C=O}$, 1500, 1572 and 1596 $\nu_{C=C}$, 1158 and 1180 $\nu_{P=N}$, 946 ν_{P-O-Ph}. ^{31}P-NMR (DMSO-d_6, ppm) $\delta = 8.25$ (3P, s, PA, A3). ^{1}H NMR (DMSO-d_6, ppm) $\delta = 3.85$ (18H, s, H^{17} ($-OCH_3$)), 3.91 (18H, s, H^{16} ($-OCH_3$)), 6.54–6.58 (12H, m, Ar–H^{12}, Ar–H^{14}), 7.12–7.14 (12H, d, $J = 7.6$ Hz, Ar–$H^{3,5}$), 7.57–7.61 (6H, d, $J = 15.6$ Hz, H^8 (–CH=)), 7.80–7.82 (6H, d, $J = 8.4$ Hz, Ar–H^{15}), 7.92–7.96 (6H, d, $J = 15.6$ Hz, H^9 (=CH–)), 7.98–8.00 (12H, d, $J = 7.6$, Ar–$H^{2,6}$). ^{13}C-APT NMR (DMSO-d_6, ppm) $\delta = 135.99$ Ar–C^1, 130.78 Ar–$C^{2,6}$, 118.76 Ar–$C^{3,5}$, 153.09 Ar–C^4, 188.10 C^7 (–C = O), 121.15 C^8 (–CH=), 139.59 C^9 (=CH–), 116.31 Ar–C^{10}, 160.43 Ar–C^{11}, 098.55 Ar–C^{12}, 163.60 Ar–C^{13}, 106.71 Ar–C^{14}, 130.47 Ar–C^{15}, 56.16 C^{16} ($-OCH_3$), 55.93 C^{17} ($-OCH_3$).

2.2.3. Synthesis of hexakis[(1-(4′-oxyphenyl)-3-(3,4-dimethoxyphenyl)prop-2-en-1-one)]cyclotriphosphazene (CP-4)

The procedure is similar to that of **CP-2**, using **HCCP** (0.2 g, 0.58 mmol), **4** (1 g, 3.49 mmol) and K_2CO_3 (0.56 g, 4.03 mmol). Yield: 76%; white solid. m.p. 189–190 °C. MALDI-MS: $N_3P_3O_{24}C_{102}H_{90}$ *m/z* calc. 1834.76; found: 1834.499 and 1857.468 [M + Na]. Microanalysis: Found: C 66.80, H 4.98%. requires C 66.77, H 4.94%. FT-IR (KBr) ν_{max} (cm^{-1}): 3001 and 3072 ν_{Ar-CH}, 2837 and 2935 $\nu_{Aliphatic-CH}$, 1653 $\nu_{C=O}$, 1512, 1575, 1594 and 1625 $\nu_{C=C}$, 1159 and 1184 $\nu_{P=N}$, 948 ν_{P-O-Ph}. ^{31}P-NMR (DMSO-d_6, ppm) $\delta = 8.21$ (3P, s, PA, A3). ^{1}H NMR (DMSO-d_6, ppm) $\delta = 3.84$ (18H, s, H^{16} ($-OCH_3$)), 3.81 (18H, s, H^{17} ($-OCH_3$)), 6.95–6.97 (6H, d, $J = 8.4$ Hz, Ar–H^{15}), 7.14–7.16 (12H, d, $J = 7.6$ Hz, Ar–$H^{3,5}$), 7.24–7.26 (6H, d, $J = 8.4$ Hz, Ar–H^{14}), 7.42 (6H, s, Ar–H^{11}), 7.62–7.65 (12H, m, H^8, H^9), 8.04–8.06 (12H, d, $J = 8.4$ Hz, Ar–$H^{2,6}$). ^{13}C-APT NMR (DMSO-d_6, ppm) $\delta = 135.74$ Ar–C^1, 130.99 Ar–$C^{2,6}$, 121.16 Ar–$C^{3,5}$, 153.22 Ar–C^4, 188.00 C^7 (–C = O), 119.31 C^8 (–CH=), 145.39 C^9 (=CH–), 137.74 Ar–C^{10}, 111.27 Ar–C^{11}, 149.34 Ar–C^{12}, 151.79 Ar–C^{13}, 111.85 Ar–C^{14}, 124.34 Ar–C^{15}, 56.02 C^{16} ($-OCH_3$), 56.06 C^{17} ($-OCH_3$).

2.2.4. Synthesis of hexakis[(1-(4′-oxyphenyl)-3-(2,3,4-trimethoxyphenyl)prop-2-en-1-one)]cyclotriphosphazene (CP-5)

The procedure is similar to that of **CP-2**, using **HCCP** (0.2 g, 0.58 mmol), **5** (1.1 g, 3.49 mmol) and K_2CO_3 (0.56 g, 4.03 mmol). Yield: 81%; white solid. m.p. 142–143 °C. MALDI-MS: $N_3P_3O_{30}C_{108}H_{102}$ *m/z* calc. 2014.92; found: 2014.306. Microanalysis: found: C 66.41, H 5.12%. requires C 64.38, H 5.10%. FT-IR (KBr) ν_{max} (cm^{-1}): 3000 and 3065 ν_{Ar-CH}, 2837 and 2938 $\nu_{Aliphatic-CH}$, 1654 $\nu_{C=O}$, 1512, 1572, 1586 and 1618 $\nu_{C=C}$, 1155 and 1180 $\nu_{P=N}$, 942 ν_{P-O-Ph}. ^{31}P-NMR (DMSO-d_6) $\delta = 8.20$ (3P, s, PA, A3). ^{1}H NMR (DMSO-d_6, ppm) $\delta = 3.75$ (18H, s, H^{18} ($-OCH_3$)), 3.79 (18H, s, H^{17} ($-OCH_3$)), 3.85 (18H, s, H^{16} ($-OCH_3$)), 6.84–6.86 (6H, d, $J = 8.8$ Hz, Ar–H^{14}), 7.14–7.16 (12H, d, $J = 8.4$ Hz, Ar–$H^{3,5}$), 7.33–7.38 (18H, m, Ar–H^{11}, Ar–H^{14}, Ar–H^{15}), 7.66–7.70 (6H, d, $J = 16$ Hz, H^8 (–CH=)), 7.70–7.73 (6H, d, $J = 8.8$ Hz, Ar–H^{15}), 7.85–7.89 (6H, d, $J = 15.6$ Hz, H^9 (=CH–)), 8.01–8.03 (12H, d, $J = 8.4$ Hz, Ar–$H^{2,6}$). ^{13}C-APT NMR (DMSO-d_6,

ppm) $\delta = 135.71$ Ar–C^{1}, 130.91 Ar–$C^{2,6}$, 121.20 Ar–$C^{3,5}$, 156.26 Ar–C^{4}, 188.01 C^{7} (–C = O), 120.09 C^{8} (–CH=), 139.17 C^{9} (=CH–), 121.32 Ar–C^{10}, 142.06 Ar–C^{11}, 153.17 Ar–C^{12}, 153.56 Ar–C^{13}, 108.74 Ar–C^{14}, 123.85 Ar–C^{15}, 61.70 C^{16} (–OCH_3), 60.86 C^{17} (–OCH_3), 56.40 C^{18} (–OCH_3).

2.2.5. Synthesis of hexakis[(1-(4′-oxyphenyl)-3-(2,4,5-trimethoxyphenyl)prop-2-en-1-one)]cyclotriphosphazene (CP-6)

The procedure is similar to that of **CP-2**, using **HCCP** (0.2 g, 0.58 mmol), **6** (1.1 g, 3.49 mmol) and K_2CO_3 (0.56 g, 4.03 mmol). Yield: 69%; white solid. m.p. 113–114 °C. MALDI-MS: $N_3P_3O_{30}C_{108}H_{102}$ *m/z* calc. 2014.92; found: 2014.224. Microanalysis: Found: C 66.42, H 5.08%. requires C 64.38, H 5.10%. FT-IR (KBr) ν_{max} (cm^{-1}): 3001 and 3065 ν_{Ar-CH}, 2834 and 2938 $\nu_{Aliphatic-CH}$, 1654 $\nu_{C=O}$, 1505, 1564 and 1597 $\nu_{C=C}$, 1158 and 1180 $\nu_{P=N}$, 945 ν_{P-O-Ph}. ^{31}P-NMR (DMSO-d_6) $\delta = 8.25$ (3P, s, PA, A3). ^{1}H NMR (DMSO-d_6, ppm) $\delta = 3.81$ (18H, s, H^{18} (–OCH_3)), 3.82 (18H, s, H^{17} (–OCH_3)), 3.87 (18H, s, H^{16} (–OCH_3)), 6.64 (6H, d, Ar–H^{12}), 7.09–7.11 (12H, d, $J = 8$ Hz, Ar–$H^{3,5}$), 7.40 (6H, s, Ar–H^{15}), 7.58–7.62 (6H, d, $J = 15.6$ Hz, H^{8} (–CH=)), 7.98–8.01 (6H, d, $J = 16$ Hz, H^{9} (=CH–)), 8.01–8.03 (12H, d, $J = 7.2$ Hz, Ar–$H^{2,6}$). ^{13}C-APT NMR (DMSO-d_6, ppm) $\delta = 136.06$ Ar–C^{1}, 130.86 Ar–$C^{2,6}$, 121.12 Ar–$C^{3,5}$, 154.78 Ar–C^{4}, 188.05 C^{7} (–C = O), 118.29 C^{8} (–CH=), 139.54 C^{9} (=CH–), 114.62 Ar–C^{10}, 143.40 Ar–C^{11}, 97.64 Ar–C^{12}, 153.38 Ar–C^{13}, 153.07 Ar–C^{14}, 111.28 Ar–C^{15}, 56.65 C^{16} (–OCH_3), 56.27 C^{17} (–OCH_3), 56.22 C^{18} (–OCH_3).

2.2.6. Synthesis of hexakis[(1-(4′-oxyphenyl)-3-(4-phenylphenyl)prop-2-en-1-one)]cyclotriphosphazene (CP-7)

The procedure is similar to that of **CP-2**, using **HCCP** (0.2 g, 0.58 mmol), **7** (1.05 g, 3.49 mmol) and K_2CO_3 (0.56 g, 4.03 mmol). Yield: 74%; white solid. m.p. 256–257 °C. MALDI-MS: $N_3P_3O_{12}C_{126}H_{90}$ *m/z* calc. 1931.04; found: 1931.561. Microanalysis: Found: C 78.39, H 4.73%. requires C 78.37, H 4.70%. FT-IR (KBr) ν_{max} (cm^{-1}): 3001 and 3065 ν_{Ar-CH}, 2834 and 2938 $\nu_{Aliphatic-CH}$, 1661 $\nu_{C=O}$, 1504, 1558 and 1597 $\nu_{C=C}$, 1161 and 1177 $\nu_{P=N}$, 969 ν_{P-O-Ph}. ^{31}P-NMR (DMSO-d_6) $\delta = 8.21$ (3P, s, PA, A3). ^{1}H NMR (DMSO-d_6, ppm) $\delta = 7.35–7.7$ (12H, d, $J = 8.4$ Hz, Ar–$H^{3,5}$), 7.41–7.42 (6H, d, Ar–H^{19}), 7.46–7.49 (12H, t, Ar–$H^{18,20}$), 7.70–7.72 (18H, m, H^{8} (–CH=) ve Ar–$H^{11,15}$), 7.73–7.78 (12H, d, Ar–$H^{12,14}$), 7.91–7.93 (12H, d, $J = 8.4$ Hz, Ar–$H^{17,21}$), 7.93–7.96 (6H, d, $J = 15.2$ Hz, H^{9} (=CH–)), 8.22–8.24 (12H, d, $J = 8.8$ Hz, Ar–$H^{2,6}$). ^{13}C-APT NMR (DMSO-d_6, ppm) $\delta = 135.58$ Ar–C^{1}, 131.28 Ar–$C^{2,6}$, 121.38 Ar–$C^{3,5}$, 153.58 Ar–C^{4}, 188.19 C^{7} (–C = O), 122.03 C^{8} (–CH=), 144.29 C^{9} (=CH–), 134.17 Ar–C^{10}, 128.47 Ar–$C^{11,15}$, 130.08 Ar–$C^{12,14}$, 142.57 Ar–C^{13}, 139.63 Ar–C^{16}, 127.19 Ar–$C^{17,21}$, 129.48 Ar–$C^{18,20}$, 127.47 Ar–C^{19}.

2.2.7. Synthesis of hexakis[(1-(4′-oxyphenyl)-3-(3,5-difluorophenyl)prop-2-en-1-one)]cyclotriphosphazene (CP-8)

The procedure is similar to that of **CP-2**, using **HCCP** (0.2 g, 0.58 mmol), **8** (0.91 g, 3.49 mmol) and K_2CO_3 (0.56 g, 4.03 mmol). Yield: 62%; white solid. m.p. 121–122 °C. MALDI-MS: $N_3P_3O_{12}C_{90}H_{54}F_{12}$ *m/z* calc. 1690.33; found: 1690.226. Microanalysis: Found: C 63.99, H 3.19%. requires C 63.95, H 3.22%. FT-IR (KBr) ν_{max} (cm^{-1}): 3005 and 3075 ν_{Ar-CH}, 2854 and 2945 $\nu_{Aliphatic-CH}$, 1667 $\nu_{C=O}$, 1502, 1595 and 1618 $\nu_{C=C}$, 1160 and 1183 $\nu_{P=N}$, 946 ν_{P-O-Ph}. ^{31}P-NMR (DMSO-d_6) $\delta = 7.93$ (3P, s, PA, A3). ^{1}H-NMR (DMSO-d_6, ppm) $\delta = 7.18–7.20$ (12H, d, $J = 8.8$ Hz, Ar–$H^{3,5}$), 7.25–7.27 (6H, Ar–H^{13}), 7.56–7.61 (18H, m, H^{8} (–CH=), Ar–H^{11}, Ar–H^{15}), 7.90–7.94 (6H, d, $J = 15.6$ Hz, H^{9} (=CH–)), 8.07–8.09 (12H, d, $J = 8.8$ Hz, Ar–$H^{2,6}$). ^{13}C-APT NMR (DMSO-d_6, ppm) $\delta = 135.01$ Ar–C^{1}, 131.31 Ar–$C^{2,6}$, 121.12 Ar–$C^{3,5}$, 153.50 Ar–C^{4}, 187.78 C^{7} (–C = O), 124.49 C^{8} (–CH=), 141.94 C^{9} (=CH–), 138.72 Ar–C^{10}, 112.26 Ar–C^{11}, 164.30 Ar–C^{12}, 105.97 Ar–C^{13}, 161.86 Ar–C^{14}, 112.26 Ar–C^{15}.

2.2.8. Synthesis of hexakis[(1-(4′-oxyphenyl)-3-(4-chloro-2-fluorophenyl)prop-2-en-1-one)]cyclotriphosphazene (CP-9)

The procedure is similar to that of **CP-2**, using **HCCP** (0.2 g, 0.58 mmol), **9** (0.97 g, 3.49 mmol) and K_2CO_3 (0.56 g, 4.03 mmol). Yield: 71%; white solid. m.p. 113–114 °C. MALDI-MS: $N_3P_3O_{12}C_{90}H_{54}F_6Cl_6$ *m/z* calc. 1789.04; found: 1789.449. Microanalysis: Found: C 60.42, H 3.04%. requires C 60.46, H 3.10%. FT-IR (KBr) ν_{max} (cm^{-1}): 3005 and 3075 ν_{Ar-CH}, 2854 and 2945 $\nu_{Aliphatic-CH}$, 1663 $\nu_{C=O}$, 1504, 1595 and 1600 $\nu_{C=C}$, 1158 and 1181 $\nu_{P=N}$, 946 ν_{P-O-Ph}. ^{31}P-NMR (DMSO-d_6) $\delta = 8.06$ (3P, s, PA, A3). ^{1}H-NMR (DMSO-d_6, ppm) $\delta = 7.16–7.18$ (12H, d, Ar–$H^{3,5}$), 7.28–7.31 (6H, d, Ar–H^{14}), 7.42–7.45 (6H, d, Ar–H^{15}), 7.61–7.65 (6H, d, $J = 16$ Hz, H^{8} (–CH=)), 7.76–7.88 (12H, m, H^{9} (=CH–), Ar–H^{12}), 7.99–8.02 (12H, d, Ar–$H^{2,6}$). ^{13}C-APT NMR (DMSO-d_6, ppm) $\delta = 134.79$ Ar–C^{1}, 131.0 Ar–$C^{2,6}$, 121.51 Ar–$C^{3,5}$, 154.06 Ar–C^{4}, 187.95 C^{7} (–C = O), 124.04 C^{8} (–CH=), 135.76 C^{9} (=CH–), 122.69 Ar–C^{10}, 162.65 Ar–C^{11}, 116.64 Ar–C^{12}, 160.15 Ar–C^{13}, 125.38 Ar–C^{14}, 129.57 Ar–C^{15}.

2.2.9. Synthesis of hexakis[(1-(4′-oxyphenyl)-3-(3-(trifluoromethyl)phenyl)prop-2-en-1-one)]cyclotriphosphazene (CP-10)

The procedure is similar to that of **CP-2**, using **HCCP** (0.2 g, 0.58 mmol), **10** (1 g, 3.49 mmol) and K_2CO_3 (0.56 g, 4.03 mmol). Yield: 79%; white solid. m.p. 115–116 °C. MALDI-MS: $N_3P_3O_{12}C_{96}H_{60}F_{18}$ *m/z* calc. 1882.44; found: 1882.555. Microanalysis: Found: C 61.29, H 3.25%. requires C 61.25, H 3.21%. FT-IR (KBr) ν_{max} (cm^{-1}): 3005 and 3075 ν_{Ar-CH}, 2854 and 2945 $\nu_{Aliphatic-CH}$, 1663 $\nu_{C=O}$, 1501, 1561 and 1598 $\nu_{C=C}$, 1157 and 1181 $\nu_{P=N}$, 957 ν_{P-O-Ph}. ^{31}P-NMR (DMSO-d_6) $\delta = 8.03$ (3P, s, PA, A3). ^{1}H-NMR (DMSO-d_6, ppm) $\delta = 7.19–7.21$ (12H, d, $J = 8.8$ Hz, Ar–$H^{3,5}$), 7.59–7.63 (6H, t, Ar–H^{14}), 7.66–7.70 (6H, d, $J = 15.6$ Hz, H^{8} (–CH=)), 7.72–7.74 (6H, d, $J = 8$ Hz, Ar–H^{13}), 7.94–7.98 (6H, d, $J = 15.6$ Hz, H^{9} (=CH–)), 8.02–8.04 (6H, d, $J = 8$ Hz, Ar–H^{15}), 8.09–8.11 (12H, d, $J = 8.8$ Hz, Ar–$H^{2,6}$), 8.15 (6H, s, Ar–H^{11}). ^{13}C-APT NMR (DMSO-d_6, ppm) $\delta = 135.11$ Ar–C^{1}, 131.31 Ar–$C^{2,6}$, 121.14 Ar–$C^{3,5}$, 153.50 Ar–C^{4}, 187.89 C^{7} (–C = O), 125.57 C^{8} (–CH=), 142.82 C^{9}

(=CH–), 136.01 Ar–C^{10}, 123.65 Ar–C^{11}, 130.00 Ar–C^{12}, 127.12 Ar–C^{13}, 130.23 Ar–C^{14}, 133.10 Ar–C^{15}, 125.80 Ar–C^{16}.

2.2.10. Synthesis of hexakis[(1-(4′-oxyphenyl)-3-(3-(trifluoromethyl)phenyl)prop-2-en-1-one)]cyclotriphosphazene (CP-11)

The procedure is similar to that of **CP-2**, using **HCCP** (0.2 g, 0.58 mmol), **11** (1.14 g, 3.49 mmol) and K_2CO_3 (0.56 g, 4.03 mmol). Yield: 81%; white solid. m.p. 159–160 °C. MALDI-MS: $N_3P_3O_{12}C_{96}H_{54}Cl_6F_{18}$ *m/z* calc. 2089.09; found: 2089.152. Microanalysis: Found: C 55.21, H 2.58%. requires C 55.19, H 2.61%. FT-IR (KBr) ν_{max} (cm^{-1}): 3045 and 3072 $\nu_{Ar\text{-}CH}$, 2898 and 2975 $\nu_{Aliphatic\text{-}CH}$, 1665 $\nu_{C=O}$, 1502 and 1599 $\nu_{C=C}$, 1160 and 1178 $\nu_{P=N}$, 950 $\nu_{P\text{-}O\text{-}Ph}$. ^{31}P-NMR (DMSO-$d_6$) $\delta = 8.01$ (3P, s, PA, A3). ^{1}H-NMR (DMSO-d_6, ppm) $\delta = 7.18$–7.20 (12H, d, $J = 8.4$ Hz, Ar–$H^{3,5}$), 7.63–7.70 (12H, m, H^8 (–CH=), Ar–H^{14}), 7.90–7.94 (12H, m, H^9 (=CH–), Ar–H^{15}), 8.06–8.08 (12H, d, $J = 8.8$ Hz, Ar–$H^{2,6}$), 8.18 (6H, s, Ar–H^{11}). ^{13}C-APT NMR (DMSO-d_6, ppm) $\delta = 132.63$ Ar–C^1, 131.29 Ar–$C^{2,6}$, 121.10 Ar–$C^{3,5}$, 153.51 Ar–C^4, 187.73 C^7 (–C = O), 128.37 C^8 (–CH=), 141.66 C^9 (=CH–), 134.64 Ar–C^{10}, 134.05 Ar–C^{11}, 127.43 Ar–C^{12}, 128.37 Ar–C^{13}, 124.15 Ar–C^{14}, 132.43 Ar–C^{15}, 124.44 Ar–C^{16}.

2.3. The frontier molecular orbitals (FMO's)

The highest occupied molecular orbital (HOMO) and the lowest unoccupied molecular orbital (LUMO) are the most important orbitals in a molecule and are called frontier moleculer orbitals (FMO's). Frontier Molecular orbitals (FMO's) generally play an essential role in chemical reactions, UV-vis spectra, optical and electrical properties (Politzer et al., 1985). Also recently, the energy gap (E_g) of HOMO-LUMO has been used to prove the chemical activity and the bioactivity from intra molecular charge transfer (Frisch et al., 2010; Politzer et al., 1985). The HOMO-LUMO energy gap and chemical reactivity identifiers were calculated using the Gaussian 09W package (Dennington & Millam, 2010) in DFT (B3LYP) methods set on the basis of 6–31G (d, p), and HOMO and LUMO images were viewed using GaussView 5.0 (Koopmans, 1934).

The ability of electron accepting and giving is defined for LUMO and HOMO, respectively. Besides, the HOMO-LUMO energies and their energy gap (Eg) are calculated with the B3LYP/6-31G(d,p) method. The global chemical reactivity and density functional descriptors of molecules such as electron affinity (A), electronegativity (χ), chemical potential (μ), ionization potential (I), global hardness (η), electrophilicity index (ω) and global softness (ζ) are calculated from the energies of the HOMO and the LUMO at B3LYP/6-31G (d,p) basis set. These parameters can be calculated as follows (Mosmann et al., 1986; Mulliken, 1934; Parr et al., 1999; Parr & Pearson, 1983; Pearson, 1985; Yang & Parr, 1985):

Energy gap, $\Delta E = E_{LUMO} - E_{HOMO}$; electron affinity, $A = -E_{LUMO}$; ionization potential, $I = -E_{HOMO}$; chemical hardness, $\eta = (I - A)/2$; chemical potential, $\mu_o = -(I + A)/2$; electronegativity, $\chi = (I + A)/2$; chemical softness, $\zeta = 1/\eta$; electrophilicity index, $\omega = \mu^2/2\eta$.

2.4. Determination of in vitro cytotoxic activity with MTT assay

In this study, *in vitro cytotoxic activities* of compounds **CP 2-11** were tested by colorimetric MTT assay against human ovarian (A2780), prostate (LNCaP and PC-3) cancer cell lines. All the cell lines were put into 25 cm^2 culture flasks containing RPMI-1640 medium (prepared using 10% FCS, 100 U/mL penicillin and 0.1 mg/mL streptomycin) and then were kept in a CO_2 incubator conditioned with 5% CO_2 at 37 °C for 24 h. The medium of cells maintained in a humid environment was changed twice a week. When cells are confluent, the cell culture medium was removed from flasks using trypsin-EDTA solution. And then the cells were transferred into to 96-well plates and used in MTT analysis. Paclitaxel and Docetaxel were used as the positive control at similar concentrations in only medium. The plates containing RPMI-1640 medium with 10% FCS, 100 U/mL penicillin and 0.1 mg/mL streptomycin were incubated at 37 °C in an incubator for 24 h. Following 24 h incubation under the same conditions, 0.5 mg/mL MTT reagent (prepared in sterile PBS) was added into 96-well plates. After waiting for 3 h in the incubator, the optical density of cells in plates were immediately read in an Elisa Microplate Reader (Synergy HT, USA) at 550 nm wavelength and the cell viability percentage of each group was calculated based on the definition of the control cell viability as 100%. Each value represents an average of 10 measurements (Görgülü et al., 2015; Morris et al., 2009; Singh & Singh, 2002). The compounds dissolved in in dimethyl sulfoxide (DMSO). The same amounts of solvent (DMSO) with 1, 5, 25, 50 and 100 μM concentrations of the compounds were added to the wells containing the cells and incubated at 37 °C for 24 h in the CO_2 incubator (Panasonic/Japan). After incubations, viability of the cells was determined using 0.4% tryphan blue in a hemocytometer.

IBM SPSS Statistics 22.0 (Windows) package program was used in Statistical Analysis. The normality distribution of the data was determined by the Shapiro Wilk test. Comparison of variables between groups was analysed with Kruskal–Wallis *H* test. Multiple Bonferroni corrected was used with Mann–Whitney *U* test. Data are expressed as mean ± standard deviation. $p < 0.05$ value was considered statistically significant. LogIC50 values were calculated using Graphpad prism 6 program in computer environment according to the obtained MTT results.

2.5. Molecular docking studies

Ligands were energy-minimized using ChemOffice on Windows 10 operating system. Grid box points as size of $96 \times 96 \times 96$ Å^3 and a regular space of 0.375 Å were determined by centring on Colchicine. "Tubulin–Colchicine complex" pdb file (PDB ID: 4O2B) was get (https://www.rcsb.org/) and was modified using the Maestro (Maestro, Schrödinger, LLC, New York, NY, 2020.). Since our compounds are large-sized molecules and the program allows up to 32 rotatable bonds, the number of rotatable bonds has been reduced to 32 for all ligands when preparing ligands with

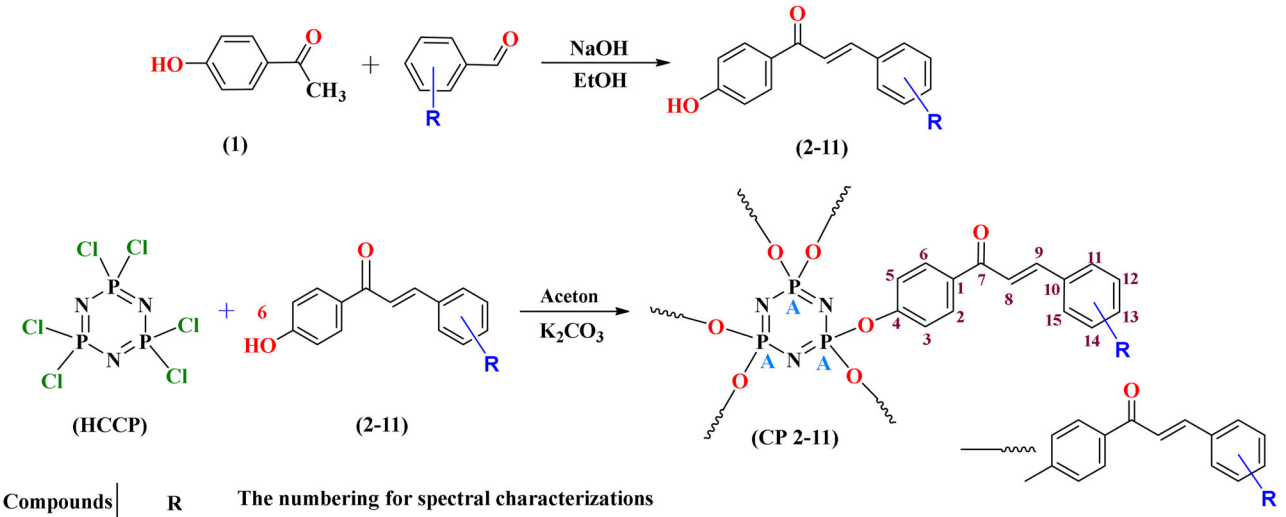

Compounds	R	The numbering for spectral characterizations
2 / CP-2	3-OCH_3	→ 3-OCH_3 --- 16,
3 / CP-3	2,4-OCH_3	→ 2-OCH_3 --- 16, 4-OCH_3 --- 17,
4 / CP-4	2,3-OCH_3	→ 2-OCH_3 --- 16, 3-OCH_3 --- 17,
5 / CP-5	2,3,4-OCH_3	→ 2-OCH_3 --- 16, 3-OCH_3 --- 17, 4-OCH_3 --- 18
6 / CP-6	2,4,5-OCH_3	→ 2-OCH_3 --- 16, 4-OCH_3 --- 17, 5-OCH_3 --- 18
7 / CP-7	4-Ph	
8 / CP-8	3,5-F	
9 / CP-9	2-F-4-Cl	
10 / CP-10	3-CF_3	→ 3-CF_3 --- 16,
11 / CP-11	3-CF_3-4-Cl	→ 3-CF_3 --- 16,

Comp. 7 and CP-7

Scheme 1 Synthetic pathway of **2-11** and **CP 2-11** and their numbering for ^{31}P, ^{1}H and ^{13}C-APT NMR characterizations

AutoDockTools4 (Trott & Olson, 2010). Docking scores were obtained using AutoDock Vina software (Table 6) (Elmas et al., 2017).

3. Results and discussion

3.1. Synthesis and characterization

The synthetic pathway of **2-11** and **CP 2-11** and their numbering for ^{31}P, ^{1}H and ^{13}C-APT NMR characterizations is shown in Scheme 1. The characteristic peaks of the compounds in the FT-IR spectrum are given in detail in the experimental section. It appears that the –OH stretching vibrations present in the starting compounds **2-11** are not observed in the FT-IR spectrum by obtaining target compounds **CP 2-11**. In addition, the peaks of the C = O stretching vibration, which is observed between 1639–1657 shift to 1653–1667 cm^{-1} in target compounds. The P = N stretching vibration peaks are seen in 1155 and 1184 cm^{-1}. The peaks of the P–O–Ph bond formed by binding the starting compounds to the cyclotriphosphazene ring were observed in the range 942–969 cm^{-1}. As a result of binding of the substituents to the trimer **(HCCP)** ring, the P = N bond is weakened and the P = N stretching vibrations of the ring have shifted to low energy.

The single peak seen in the ^{31}P-NMR spectra shows that the phosphorous in the structure have the same chemical environment, symmetrical structure and the spin system is in the form of A3. When the ^{31}P-NMR spectra were examined, the structure formed was symmetrical and the peak of equivalent phosphorous observed at 21.12 ppm belonging to the trimer **(HCCP)** was not observed by obtaining the target compounds **CP 2-11**. As a result of obtaining the target compounds, phosphorus peaks were observed as singlets in the range 7.93–8.25 ppm for each compound. In addition, the phosphorus peak has shifted to the high field due to the substitution effect attached to the phosphazene ring. This means that the electron density on the phosphorus atom increases. This can be explained by the fact that the substituent attached to the phosphazene ring attracts electrons, causing the electrons in the P = N bond to intensify on the phosphorous.

A proton –OH peaks observed in the range 10.29–10.52 ppm in the ^{1}H-NMR spectra of the starting compounds **2-11** were not observed in after formation of target products **CP 2-11**. This is the first proof that substitution has occurred. The olefin proton peaks of the starting compounds at 7.63–7.80 (1H, d, J = 15.6 Hz) and 7.79–8.14 (1H, d, J = 15.6 Hz) ppm were shifted to 7.57–7.70 (6H, d, J = 15.6, H^8) and 7.70–8.01 (6H, d, J = 15.6, H^9) ppm ranges after the formation of target compounds. In addition, the obtained integral heights are compatible with the structure and the aromatic (for **CP 2-11**) and aliphatic (for **CP 2-6**) protons in the structure of the starting compounds are observed with low shifts and changes in the protons next to the phosphorus atom are the proof for formation of the target structure.

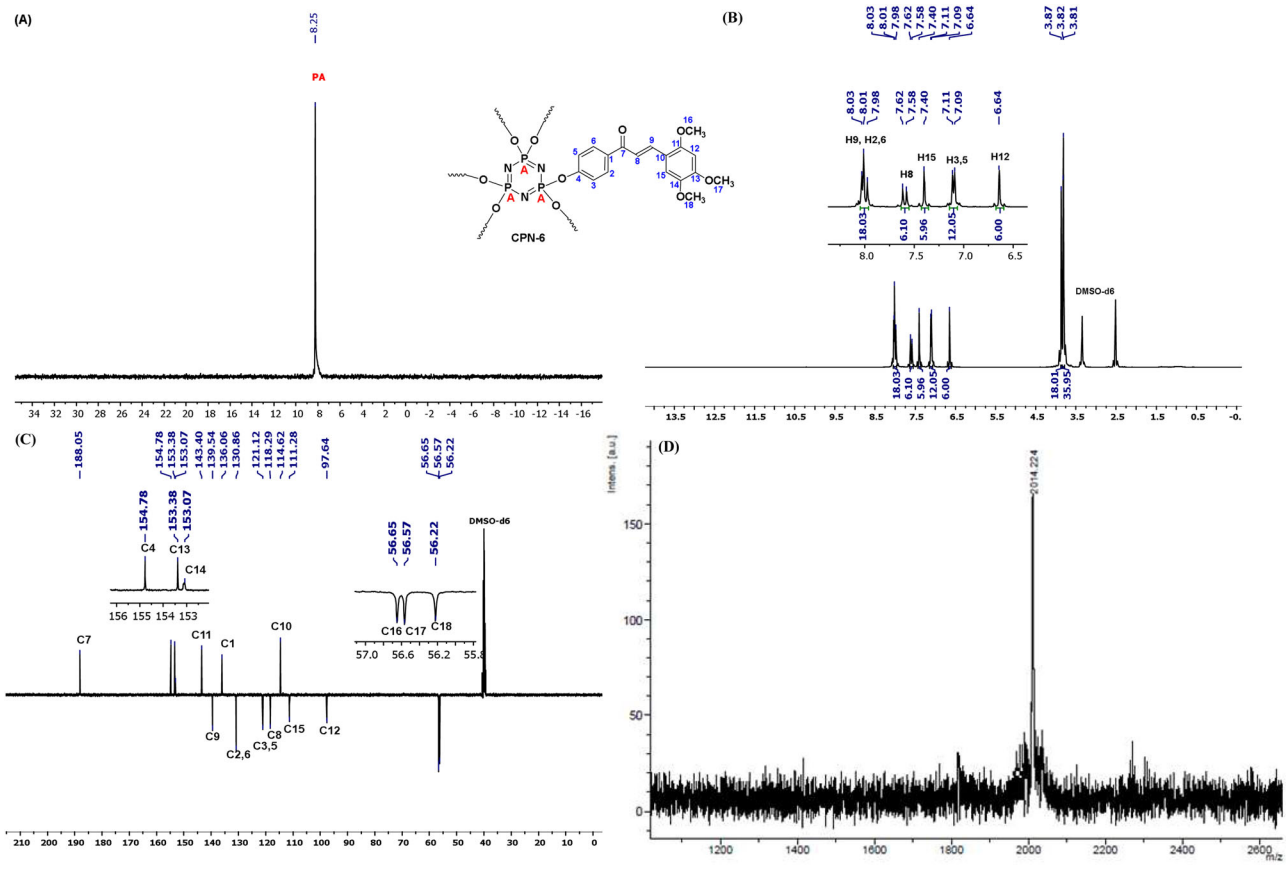

Figure 1. (A) ^{31}P, (B) ^{1}H and (C) ^{13}C-APT NMR spectrum in DMSO-d_6 and (D) MALDI-TOF MS spectrum of compound **CP-6**.

Table 1. TGA data for the decomposition and DSC values of compounds **CP 2-11**.

Compounds CP 2-11	TGA results			DSC results Melting point
	T_i (°C)[a]	$T_{50\%}$ (°C)[b]	Residue (%, 800 °C)	
CP-2	306.15	664.28	26.44	125–126
CP-3	329.41	654.73	20.66	135–136
CP-4	311.14	613.81	19.72	189–190
CP-5	331.46	643.14	18.44	142–143
CP-6	318.50	629.50	19.17	113–114
CP-7	321.91	648.59	21.82	256–257
CP-8	261.21	614.49	17.52	121–122
CP-9	290.54	613.13	22.15	113–114
CP-10	293.27	564.02	28.42	115–116
CP-11	290.54	570.84	18.07	159–160

[a]Initial decomposition temperature.
[b]Decomposition temperature at 50% mass loss.

In the ^{13}C-APT NMR spectrum of the compounds, C = O carbon was seen in the range 187.16–187.69 ppm (C8) for the starting compounds **2-11**, while this peak shifted to the range 187.73–188.19 ppm (C7) in the target compounds **CP 2-11**. This situation shows the change of the structure after it is bounded to the phosphazene ring. While the ipso carbon (C4) of the starting compounds bound to the –OH group was observed in the range 162.32–163.28 ppm, this carbon peak shifted to the range 153.09–156.26 ppm (C4) after binding to the cyclotriphosphazene ring. This is an indication that formation of substitution is based on the result from the ^{13}C-APT NMR spectrum. Apart from these examples, it is seen that there are significant shifts in carbon peaks due to interactions in other carbon atoms.

The experimental values of the compounds in the MALDI-TOF MS spectrum appear to be almost exactly the same as the theoretically calculated values. This is one of the most important evidence that the compounds are formed (Figure 1).

The thermal characteristics of the target compounds were determined by thermogravimetric analysis (TGA), and the results showed that the compounds are highly stable to high temperatures. Detailed results are given in Table 1.

3.2. The determination of frontier molecular orbitals (FMO's)

The HOMO-LUMO energy gap and chemical reactivity identifiers for **CP 2-11** were calculated using the Gaussian 09W package in DFT (B3LYP) methods set on the basis of 6-31G (d, p), and HOMO and LUMO images were viewed using GaussView 5.0. The 3D plots of the HOMO and LUMO orbitals of molecules were shown in Figure 2. As can be seen in Figure 2, there is a charge transfer within the molecules. The results of E_{LUMO}, E_{HOMO}, E_g, electron affinity, ionization potential, chemical softness, chemical potential, chemical hardness, electrophilicity index and electronegativity parameters for **CP 2-11** are given in Table 2 according to the obtained calculations.

When the chemical hardness is considered, a molecule having a small HOMO–LUMO energy gap means a soft

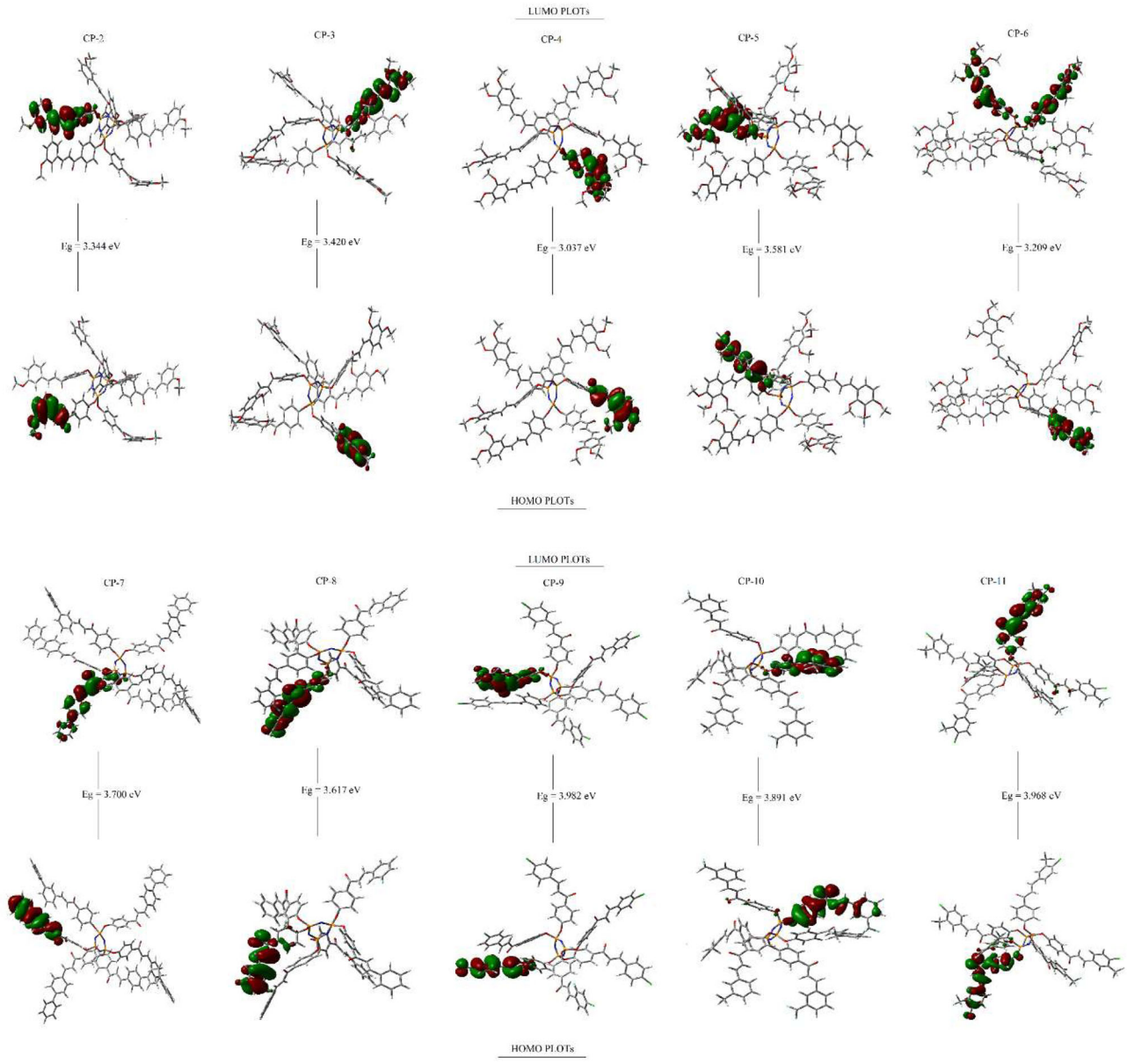

Figure 2. Molecular orbital representation of the molecules **(CP 2-11)**.

Table 2. Some electronic structure parameters for the molecules **(CP 2-11)** calculated at B3LYP/6-31G (d,p) basis set.

	Values (eV)									
Parameters	CP-2	CP-3	CP-4	CP-5	CP-6	CP-7	CP-8	CP-9	CP-10	CP-11
E_{LUMO}	−2.3845	−1.9575	−2.2218	−2.0511	−1.9080	−2.2035	−2.8041	−2.4174	−2.7195	−2.7535
E_{HOMO}	−5.7290	−5.3783	−5.2591	−5.6330	−5.1173	−5.9040	−6.4218	−6.3998	−6.6107	−6.7217
E_g	3.3445	3.4207	3.0373	3.5818	3.2093	3.7005	3.6177	3.9824	3.8912	3.9682
A	2.3845	1.9575	2.2218	2.0511	1.9080	2.2035	2.8041	2.4174	2.7195	2.7535
I	5.7290	5.3783	5.2591	5.6330	5.1173	5.9040	6.4218	6.3998	6.6107	6.7217
Z	0.5980	0.5846	0.6585	0.5583	0.6232	0.5404	0.5528	0.5022	0.5139	0.5040
M	−4.0567	−3.6679	−3.7404	−3.8420	−3.5126	−4.0537	−4.6129	−4.4086	−4.6651	−4.7376
H	1.6722	1.7103	1.5186	1.7909	1.6046	1.8502	1.8088	1.9912	1.9456	1.9841
Ω	4.9205	3.9329	4.6062	4.1211	3.8445	4.4406	5.8818	4.8804	5.5929	5.6561
X	4.0567	3.6679	3.7404	3.8420	3.5126	4.0537	4.6129	4.4086	4.6651	4.7376

$E_g = E_{LUMO} - E_{HOMO}$; *A*, electron affinity; I, ionization potential; ζ, chemical softness; μ, chemical potential; η, chemical hardness; ω, electrophilicity index; χ, electronegativity.

molecule and large energy gap means a hard molecule. It may also relate to the stability of the molecule against hardness. That is, the molecule with least energy gap is less stable and more reactive. The calculated energy gap values of **CP 2-11** molecules are 3.34, 3.42, 3.03, 3.58, 3.20, 3.70, 3.61, 3.98, 3.89 and 3.96 eV, respectively. Taking into account the values of the energy between HOMO and LUMO, it is shown that the energy gap of **CP-4** molecule smaller than the other

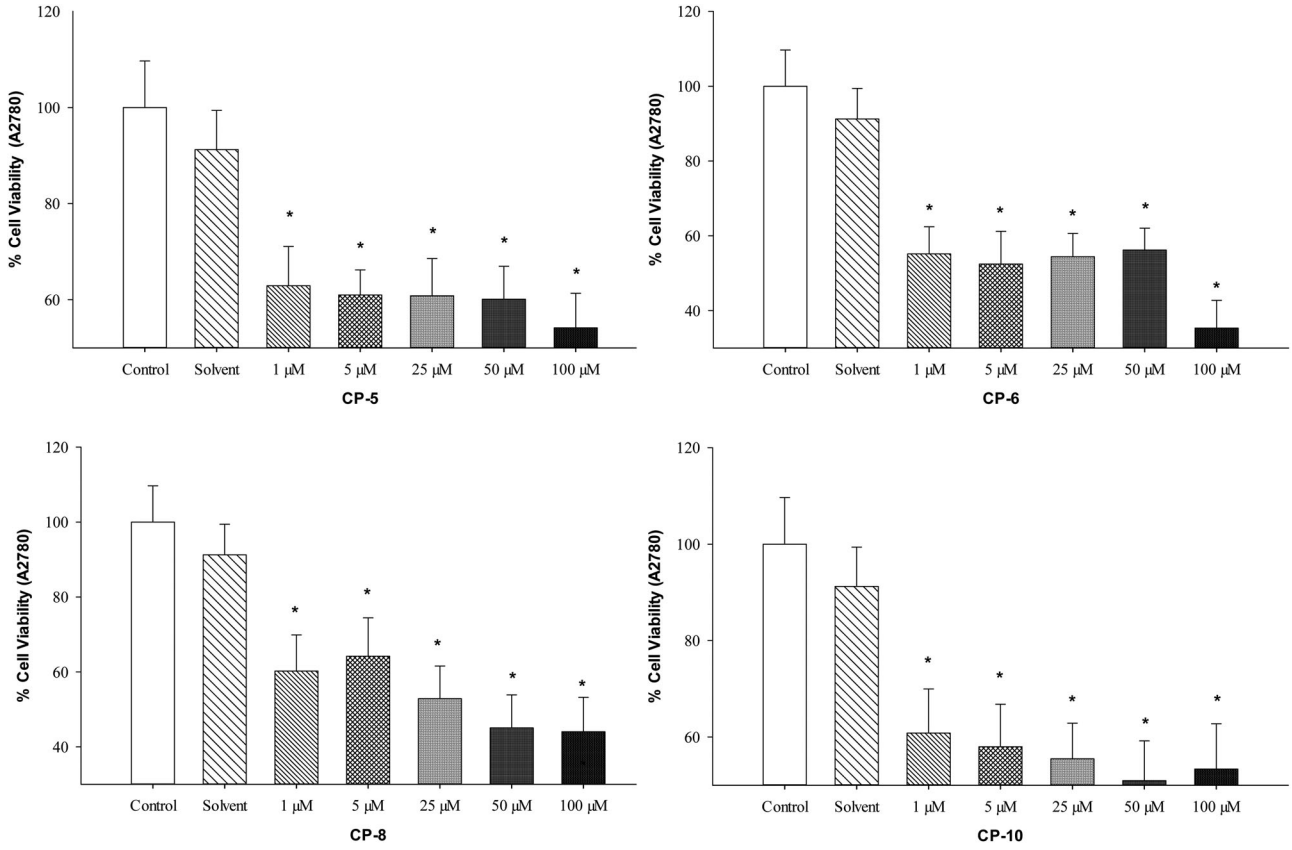

Figure 3. The cell viability results of PC-3 cells after a 24-h treatment with **CP-5**, **CP-6**, **CP-8** and **CP-10**. The changes on the cell viability (%) caused by hexa substituted cyclotriphosphazene derivatives are compared with the control data. Each data point is an average of 10 viabilities ($^*p < 0.05$).

molecules. That is, this molecule is less stable and more reactive than others. Besides, as shown in Table 2, all the chemical potential values are negative and it means that the molecules are stable.

3.3. In vitro cytotoxic activity

3.3.1. Cytotoxicity of the compounds on cell lines

In vitro cytotoxic activities of **CP 2-11** were analysed via MTT assay against human ovarian (A2780), prostate (LNCaP and PC-3) cancer cell lines. The percentages of viable cells were determined at different concentrations (1, 5, 25, 50 and 100 μM).

The articles on the cytotoxic activity of substituted phosphazene compounds against different cancer cells are available in the literature (Akbaş et al., 2013; Binici et al., 2019; Görgülü et al., 2015; Tümer et al., 2018). In these studies, it is stated that the substituted phosphazene compounds show significant cytotoxic effects. In addition, toxic effects of compounds against normal cells were investigated and it has been found that substituted phosphazene compounds do not show toxic effects (Koran et al., 2017). It is stated in the literature that degradation products of phosphazene compounds are non-toxic (Andrianov, 2008). In conclusion, these compounds can be expressed as strong candidate molecules for pharmaceutical applications.

In terms of MTT results, compounds **CP 2-11** appear to be highly effective at high doses ($^*p < 0.05$). Applied compounds **CP 2-11**, except **CP 3**, **4** and **11**, showed significant cytotoxic effect on A2780 cell lines at different concentrations ($^*p < 0.05$). Compound **CP 3**, **4** and **11** were exhibited significant cytotoxic effect on the cell viability at only 100 μM concentration ($^*p < 0.05$). The cell viability of compounds **CP 5, 6, 8** and **10** against A2780 cells decreased in a dose-dependent manner (Figure 3 and Table 3, $^*p < 0.05$). All concentrations of these compounds showed significant cytotoxic effect ($^*p < 0.05$). At 25, 50 and 100 μM concentrations for compound **CP-2**, at 50 and 100 μM concentrations for compound **CP-7** and at 5, 25, 50 and 100 μM concentrations for compound **CP-9** were exhibited significant cytotoxic effect (Table 3, $^*p < 0.05$).

The results of **CPN 2-11** on human prostate cancer cell lines are given in Table 4. When the cytotoxic activities of target compounds against human prostate cancer cell lines are examined, compounds **CPN-2**, **3**, **6** and **7** have been significantly reduced cell viability in a dose-dependent manner against the PC-3 cell lines at all concentrations ($^*p < 0.05$). The graphics of **CPN-2**, **3**, **6** and **7** showing dose-dependent effects are given in Figure 4.

At only 100 μM concentration for **CP-2** and **CP-6**, at 25, 50 and 100 μM concentrations for **CP-3**, at 50 and 100 μM concentrations for **CP-7** were exhibited significant cytotoxic effect against LNCaP cancer cell lines ($^*p < 0.05$). Compounds **CPN-8**, has been significantly reduced cell viability in a dose-dependent manner against the LNCaP cell lines at all concentrations ($^*p < 0.05$). The $\log IC_{50}/IC_{50}$ values of **CP 2-11** against all cancer cell lines are given in Table 5.

Table 3. % Cell viability of compounds CP 2-11 against human ovarian cancer cell lines (*$p < 0.05$).

A2780 human ovarian cancer cell lines							
	Control	Solvent	1 μM	5 μM	25 μM	50 μM	100 μM
CP-2	100 ± 9.67	91.25 ± 8.16	86.23 ± 12.63	88.02 ± 7.99	69.22 ± 6.91*	60.23 ± 9.12*	30.14 ± 5.81*
CP-3	100 ± 9.67	91.25 ± 8.16	90.14 ± 12.69	92.68 ± 15.76	88.16 ± 19.8	91.71 ± 10.16	26.43 ± 7.96*
CP-4	100 ± 9.67	91.25 ± 8.16	92.26 ± 10.33	100.84 ± 15.6	93.64 ± 10.9	98.75 ± 8.29	7.23 ± 1.09*
CP-5	100 ± 9.67	91.25 ± 8.16	62.93 ± 8.16*	60.99 ± 5.23*	60.83 ± 7.75*	60.13 ± 6.83*	54.16 ± 7.19*
CP-6	100 ± 9.67	91.25 ± 8.16	55.15 ± 7.26*	52.45 ± 8.72*	54.40 ± 6.23*	56.19 ± 5.86*	35.32 ± 7.41*
CP-7	100 ± 9.67	91.25 ± 8.16	93.26 ± 10.26	89.26 ± 11.06	90.26 ± 9.12	66.31 ± 6.19*	32.16 ± 2.36*
CP-8	100 ± 9.67	91.25 ± 8.16	60.21 ± 9.66*	64.19 ± 10.22*	52.86 ± 8.69*	45.06 ± 8.81*	44.03 ± 9.17*
CP-9	100 ± 9.67	91.25 ± 8.16	82.42 ± 11.26	62.19 ± 8.12*	41.21 ± 7.26*	30.81 ± 6.03*	22.09 ± 5.74*
CP-10	100 ± 9.67	91.25 ± 8.16	60.81 ± 9.16*	58.00 ± 8.81*	55.48 ± 7.39*	50.96 ± 8.24*	53.35 ± 9.41*
CP-11	100 ± 9.67	91.25 ± 8.16	79.50 ± 9.23	81.34 ± 10.41	79.83 ± 7.06	80.20 ± 10.92	52.31 ± 8.81*

μM, micromolar.
*It is statistically significant.

Table 4. % Cell viability of compounds CP 2-11 against human prostate cancer cell lines (*$p < 0.05$).

LNCaP human prostate cancer cell lines							
	Control	Solvent	1 μM	5 μM	25 μM	50 μM	100 μM
CP-2	100 ± 8.99	93.17 ± 10.12	96.58 ± 11.8	84.05 ± 10.29	80.94 ± 9.33	88.06 ± 9.67	44.30 ± 10.21*
CP-3	100 ± 8.99	93.17 ± 10.12	92.26 ± 9.23	73.08 ± 10.12	62.75 ± 6.15*	61.03 ± 5.23*	57.91 ± 8.81*
CP-4	100 ± 8.99	93.17 ± 10.12	97.41 ± 8.26	84.93 ± 10.13	80.08 ± 9.64	70.39 ± 5.12*	62.21 ± 7.26*
CP-5	100 ± 8.99	93.17 ± 10.12	87.06 ± 8.29	77.74 ± 11.16	72.25 ± 10.2	63.56 ± 8.85*	63.87 ± 6.69*
CP-6	100 ± 8.99	93.17 ± 10.12	95.13 ± 8.21	83.43 ± 7.46	72.56 ± 9.21	72.04 ± 12.36	55.73 ± 8.17*
CP-7	100 ± 8.99	93.17 ± 10.12	100.02 ± 14.	108.85 ± 16.2	93.31 ± 12.3	44.11 ± 8.77*	11.38 ± 2.41*
CP-8	100 ± 8.99	93.17 ± 10.12	68.29 ± 8.69*	69.96 ± 6.78*	63.14 ± 9.12*	67.27 ± 7.45*	63.84 ± 8.88*
CP-9	100 ± 8.99	93.17 ± 10.12	76.12 ± 10.2	51.39 ± 8.99*	39.48 ± 9.26*	39.69 ± 10.13*	31.12 ± 7.94*
CP-10	100 ± 8.99	93.17 ± 10.12	94.33 ± 6.69	91.44 ± 8.22	77.04 ± 8.19	63.38 ± 7.25*	50.83 ± 10.16*
CP-11	100 ± 8.99	93.17 ± 10.12	88.10 ± 9.26	77.69 ± 7.26	75.92 ± 10.8	68.49 ± 6.90*	62.54 ± 8.19*
PC-3 human prostate cancer cell lines							
	Control	Solvent	1 μM	5 μM	25 μM	50 μM	100 μM
CP-2	100 ± 9.13	92.36 ± 8.13	72.97 ± 6.89*	65.87 ± 6.13*	60.78 ± 5.94*	65.16 ± 6.44*	35.13 ± 4.11*
CP-3	100 ± 9.13	92.36 ± 8.13	60.42 ± 7.29*	56.73 ± 5.69*	50.72 ± 10.14*	48.59 ± 8.91*	18.49 ± 3.51*
CP-4	100 ± 9.13	92.36 ± 8.13	94.49 ± 10.2	91.22 ± 12.51	102.56 ± 18.4	37.39 ± 6.29*	11.64 ± 4.52*
CP-5	100 ± 9.13	92.36 ± 8.13	96.21 ± 12.6	100.03 ± 13.2	85.16 ± 10.81	52.26 ± 7.19*	10.91 ± 2.76*
CP-6	100 ± 9.13	92.36 ± 8.13	54.60 ± 5.23*	50.98 ± 6.21*	52.61 ± 5.26*	47.65 ± 8.17*	20.54 ± 2.29*
CP-7	100 ± 9.13	92.36 ± 8.13	40.73 ± 6.72*	40.44 ± 7.94*	47.49 ± 8.90*	47.96 ± 9.41*	45.26 ± 5.36*
CP-8	100 ± 9.13	92.36 ± 8.13	76.68 ± 9.32	73.63 ± 7.22*	71.06 ± 6.49*	52.74 ± 7.93*	28.58 ± 4.38*
CP-9	100 ± 9.13	92.36 ± 8.13	90.06 ± 8.74	82.95 ± 9.34	74.10 ± 10.41	69.39 ± 7.32*	31.34 ± 3.41*
CP-10	100 ± 9.13	92.36 ± 8.13	95.64 ± 5.36	105.06 ± 8.91	105.09 ± 12.7	97.49 ± 16.6	39.06 ± 5.29*
CP-11	100 ± 9.13	92.36 ± 8.13	108.47 ± 5.3	106.81 ± 12.0	109.11 ± 18.8	101.68 ± 14.4	64.17 ± 8.91*

μM, micromolar.
*It is statistically significant.

When the cytotoxic activity results of the target compounds **CP 2-11** on human prostate cancer cell lines were examined, **CP 2-11** were more effective against PC-3 cancer cell lines. According to the information given above, some substances have a cytotoxic effect against PC-3 cell lines at almost all concentrations, whereas the same effect has not been observed against LNCaP cell lines (e.g. **CP-2** compound). Against this cell line, **CP 2-11** compounds generally showed high doses of cytotoxic effects.

In this study, it was observed that there were significant differences in cell viability compared to the cytotoxicity activity results of the disubstituted and tetra-substituted phosphazene compounds of the hexa-substituted phosphazene compounds with the cytotoxic activities of our study team. In our previous study, the cytotoxicity activity results of disubstituted and tetra substituted phosphazene containing different organic groups were compared with the results of hexa-substituted phosphazene in this study and it was determined that there were significant differences in cell viability (Görgülü et al., 2015; Koran, Tekin, Biryan, et al., 2017; Koran Tekin, Çalışkan, et al., 2017). While the dose-dependent effect was not observed in the compounds used in previous studies, most of the compounds in hexa-substituted structures decreased dose-dependent cell viability. Also, in previous studies, the compounds generally showed a high dose (100 μM) cytotoxic effect. While the results obtained in previous studies caused a decrease in cell viability by 50%–60% at this dose, the results in our current study showed that the decrease in cell viability was 70%–90% (e.g. **CP 2-4, CP-7, 8**).

3.4. Molecular docking studies

According to the X-ray crystallographic structure of Tubulin–Colchicine complex (PDB ID:4O2B), main binding site has been determined around Colchicine (Ligand ID: LOC) and Guanosine-5′-Triphosphate (Ligand ID: GTP) in receptor (https://www.rcsb.org/). It has been declared that colchicine interacts with active site in tubulin as binding site. It has

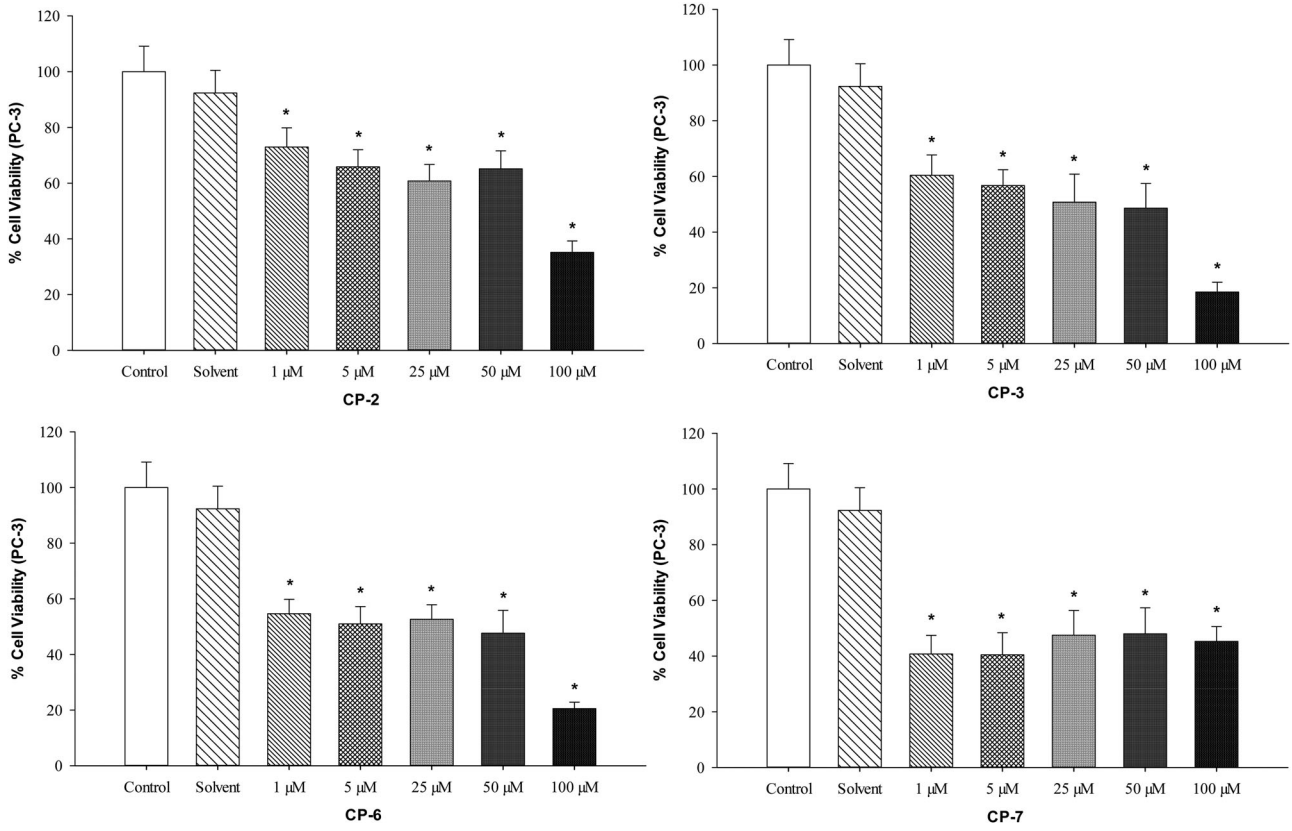

Figure 4. The cell viability results of PC-3 cells after a 24-h treatment with **CP-2**, **CP-3**, **CP-6** and **CP-7**. The changes on the cell viability (%) caused by hexa substituted cyclotriphosphazene derivatives are compared with the control data. Each data point is an average of 10 viabilities ($^{*}p < 0.05$).

Table 5. LogIC_{50}/IC_{50} (50% inhibition-causing concentration) values (μM) of CP 2-11 against human ovarian (A2780) and prostate (LNCaP, and PC-3) cancer cell lines.

Comp.	A2780 LogIC_{50}/IC_{50} (μM)	LNCaP LogIC_{50}/IC_{50} (μM)	PC-3 LogIC_{50}/IC_{50} (μM)
CP-2	1.749/56.1	2.09/123.2	1.709/51.13
CP-3	2.021/104.9	1.886/76.98	1.326/21.2
CP-4	1.971/93.62	2.118/131.1	1.698/49.87
CP-5	1.794/62.25	2.023/105.3	1.707/50.98
CP-6	1.524/33.41	2.029/106.9	1.297/19.82
CP-7	1.911/81.44	1.721/52.56	1.285/19.28
CP-8	1.526/33.57	1.978/95.15	1.665/46.23
CP-9	1.182/15.22	1.174/14.92	1.835/68.34
CP-10	1.652/44.86	1.961/91.45	2.237/172.5
CP-11	2.089/122.9	2.07/117.6	2.571/372.4
Paclitaxel	0.7516/5.645	–	–
Docetaxel	–	0.7792/6.014	1.229/16.95

μM, micromolar.

been previously established that colchicine interacts with SER178A, THR179A, ALA180A, VAL181A, CYS241B, LEU242B, LEU248B, ALA250B, ASP251B, LYS254B, LEU255B, ASN258B, MET259B, THR314B, VAL315B, ALA316B, ILE318B, ASN350B, LYS352B, ILE378B residues (https://www.ebi.ac.uk/pdbe/). Hydrophobic, H-bond, Pi–Pi stacking, Pi-cation, Halogen bond interactions of all ligands were given in detail with interacting residues (Table 6).

Docking studies were performed for the all compounds. Interaction modes for compounds **CP 2-11** with enzyme active sites were determined. 2D Interaction diagram for compound **CP-5** and **CP-6** at the Tubulin-binding cavity are given in Figure 5. The binding types and residues were produced showed by Maestro software (Maestro, Schrödinger, LLC, New York, NY, 2020). Binding modes of these compounds were revealed to be similar to colchicine, but it was found that these large chemical structured ligands did not settle inside the receptor and were docked externally with the corresponding residues (Figure 6).

4. Conclusion

In conclusion, a new series hexa substituted cyclicphosphazenes **CP 2-11** obtained and their investigated *in vitro* cytotoxicity properties, theoretical analysis and molecular docking studies. The structures of **CP 2-11** were characterized using ^{31}P, ^{1}H-NMR, ^{13}C-APT NMR, FT-IR and MALTI-TOF MS spectroscopic methods. In addition, thermal stability of the compounds was determined by taking DSC and TGA thermograms. The HOMO-LUMO energy gap and chemical reactivity identifiers were calculated and HOMO and LUMO images were viewed. According to the calculations, all the chemical potential values of **CP 2-11** are negative and it shown that the molecules are stable. Molecular docking studies exhibited the interaction mode of all compounds with tubulin including some hydrophobic, H-bond, Pi–Pi stacking, Pi-cation, Halogen bond interactions. In the last step, hexa substituted cyclotrophosphazenes **CP 2-11** at different concentrations (1, 5, 25 and 50 μM) are employed against human ovarian (A2780) and human prostate (PC-3 and LNCaP) cancer cell lines to investigate % cell viability and *in vitro* cytotoxicity activities using the MTT assay method. **CP 2-11**

Table 6. Molecular docking-binding scores of **CP 2-11**, within the Tubulin-Colchicine complex (PDB ID: 4O2B) active site.

	Residues participating				
Comp.	H-bond	Pi–Pi stacking	Pi-cation	Halogen bond	Best docking score
CP-2	ASN18A SER178A TYR224A THR225A	TYR224A	ARG229A	–	–9.2
CP-3	THR82A ARG229A GLY246B	–	–	–	–11.1
CP-4	ARG214A GLN336B	HIS393A	LYS352B	–	–10.6
CP-5	ASN18A	TYR224A	–	–	–11.3
CP-6	ARG253B	–	ARG158B ARG164B ARG253B	–	–10.8
CP-7	ARG229A	–	ARG229A	–	–8.9
CP-8	–	TYR108A TRP407A	ARG164B	–	–10.3
CP-9	ASN228A	–	ARG229A	THR82A ARG84A	–9.6
CP-10	LEU132B	–	ARG121A	–	–8.3
CP-11	–	–	LYS304A LYS394A	GLU429A PHE343B VAL344B	–11.6

nM, nanomolar; μM, micromolar.
Residues participating H-bond, Pi–Pi stacking, Pi-cation, halogen-bond interactions with the compounds are shown.

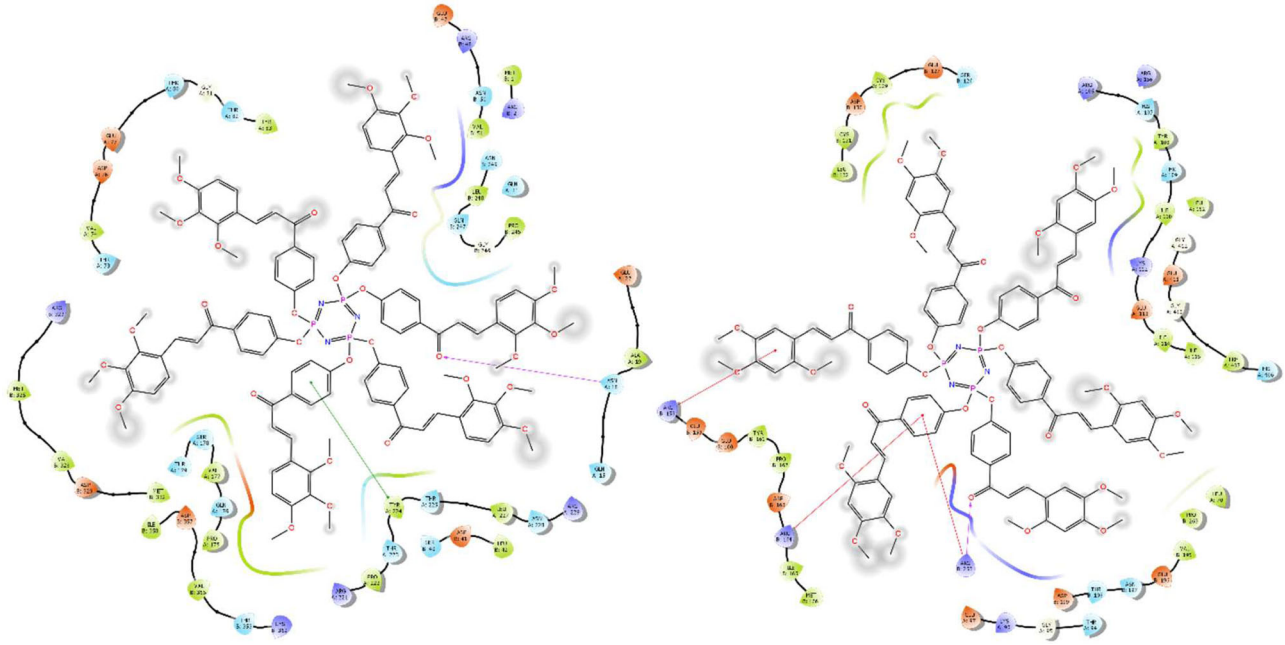

Figure 5. 2D interaction diagram for compounds **CP-5 and CP-6** at the Tubulin-binding cavity, respectively.

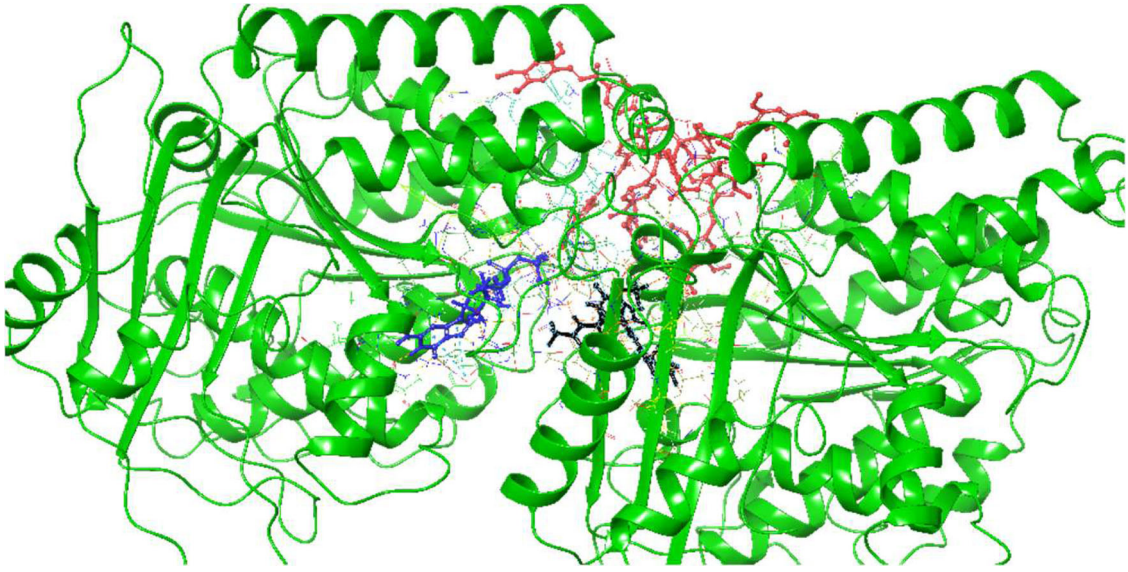

Figure 6. The positioning of **CP-6** (red), Colchicine (black) and Guanosine-5′-Triphosphate (blue) compounds with in Tubulin-Colchicine complex (green) was presented.

compounds were found to demonstrate cytotoxic activity against these human cancer cell lines. The results showed that the decrease in cell viability was 70%–90% (e.g. **CP 2-4, CP-7, 8**) and these compounds are powerful candidate molecules for pharmaceutical applications.

Acknowledgements

The author would like to thank Bingöl University for the server and Bitlis Eren University for Gaussian software.

Disclosure statement

No potential conflict of interest was reported by the authors.

Funding

The Scientific and Technological Research Council of TurkeyThis work was supported by a grant from The Scientific and Technological Research Council of Turkey (Grant No: 116Z758).

ORCID

Harun Uslu http://orcid.org/0000-0001-8827-8557
Süleyman Sandal http://orcid.org/0000-0002-8916-3329

References

Akbaş, H., Okumuş, A., Kılıç, Z., Hökelek, T., Süzen, Y., Koç, L. Y., Açık, L., & Çelik, Z. B. (2013). Phosphorus-nitrogen compounds part 27. Syntheses, structural characterizations, antimicrobial and cytotoxic activities, and DNA interactions of new phosphazenes bearing secondary amino and pendant (4-fluorobenzyl)spiro groups. *European Journal of Medicinal Chemistry*, *70*, 294–307. https://doi.org/10.1016/j.ejmech.2013.09.046

Alidağı, H. A., Gırgıç, Ö. M., Zorlu, Y., Hacıvelioğlu, F., Çelik, S. Ü., Bozkurt, A., Kılıç, A., & Yeşilot, S. (2013). Synthesis and proton conductivity of azole-substituted cyclic and polymeric phosphazenes. Polymer, *54*(9), 2250–2256.

Allcock, H. R. (1972). *Phosphorus-nitrogen compounds; cyclic, linear, and high polymeric systems*. Academic Press.

Andrianov, A. K. (2008). *Polyphosphazenes for medical applications*. John Wiley & Sons, Inc.

Asmafiliz, N., Berberoğlu, İ., Özgür, M., Kılıç, Z., Kayalak, H., Açık, L., Türk, M., & Hökelek, T. (2019). Phosphorus-nitrogen compounds: Part 46. The reactions of N3P3Cl6 with bidentate and monodentate ligands: The syntheses, structural characterizations, antimicrobial and cytotoxic activities, and DNA interactions of (N/N)spirocyclotriphosphazenes with 4-chlorobenzyl pendant arm. *Inorganica Chimica Acta*, *495*, 118949.

Binici, A., Okumuş, A., Elmas, G., Kılıç, Z., Ramazanoğlu, N., Açık, L., Şimşek, H., Çağdaş Tunalı, B., Türk, M., Güzel, R., & Hökelek, T. (2019). Phosphorus–nitrogen compounds. Part 42. The comparative syntheses of 2-cis-4-ansa(N/O) and spiro(N/O) cyclotetraphosphazene derivatives: Spectroscopic and crystallographic characterization, antituberculosis and cytotoxic activity studies. *New Journal of Chemistry*, *43*(18), 6856–6873.

Bist, G., Pun, N. T., Magar, T. B. T., Shrestha, A., Oh, H. J., Khakurel, A., Park, P.-H., & Lee, E.-S. (2017). Inhibition of LPS-stimulated ROS production by fluorinated and hydroxylated chalcones in RAW 264.7 macrophages with structure-activity relationship study. *Bioorganic & Medicinal Chemistry Letters*, *27*(5), 1205–1209. https://doi.org/10.1016/j.bmcl.2017.01.061

Bobrov, M. F., Buzin, M. I., Primakov, P. V., & Chistyakov, E. M. (2020). Investigation of hexakis[2-formylphenoxy]cyclotriphosphazene structure by single crystal X-ray diffraction and computer simulation. *Journal of Molecular Structure*, *1208*, 127896.

Bolink, H. J., Barea, E., Costa, R. D., Coronado, E., Sudhakar, S., Zhen, C., & Sellinger, A. (2008). Efficient blue emitting organic light emitting diodes based on fluorescent solution processable cyclic phosphazenes. *Organic Electronics*, *9*(2), 155–163.

Brian, A. J., Furniss, H. S., Smith, P. W. G., & Tatchell, A. R. (1989). *Vogel's textbook of practical organic chemistry, Longman scientific technical*. John Wiley Sons, Inc.

Carlson, R. O. (2008). New tubulin targeting agents currently in clinical development. *Expert Opinion on Investigational Drugs*, *17*(5), 707–722. https://doi.org/10.1517/13543784.17.5.707

Carriedo, G. A., Fernández-Catuxo, L., García Alonso, F. J., Gómez-Elipe, P., & González, P. A. (1996). Preparation of a new type of phosphazene high polymers containing 2,2'-dioxybiphenyl groups. Macromolecules, *29*(16), 5320–5325.

Chaudhary, M., Kumar, N., Baldi, A., Chandra, R., Arockia Babu, M., & Madan, J. (2020). Chloro and bromo-pyrazole curcumin Knoevenagel condensates augmented anticancer activity against human cervical cancer cells: Design, synthesis, in silico docking and in vitro cytotoxicity analysis. *Journal of Biomolecular Structure & Dynamics*, *38*(1), 200–218.

Chen, J., Wang, L., Fan, Y., Yang, Y., Xu, M., & Shi, X. (2019). Synthesis and anticancer activity of cyclotriphosphazenes functionalized with 4-methyl-7-hydroxycoumarin. *New Journal of Chemistry* , *43*(46), 18316–18321.

Chimenti, F., Bolasco, A., Manna, F., Secci, D., Chimenti, P., Befani, O., Turini, P., Giovannini, V., Mondovì, B., Cirilli, R., & Torre, F. L. (2004). Synthesis and selective inhibitory activity of 1-acetyl-3,5-diphenyl-4,5-dihydro-(1H)-pyrazole derivatives against monoamine oxidase. *Journal of Medicinal Chemistry*, *47*(8), 2071–2074. https://doi.org/10.1021/jm031042b

Çoşut, B., Hacıvelioğlu, F., Durmuş, M., Kılıç, A., & Yeşilot, S. (2009). The synthesis, thermal and photophysical properties of phenoxycyclotriphosphazenyl-substituted cyclic and polymeric phosphazenes. Polyhedron, *28*(12), 2510–2516.

Dagdag, O., El Harfi, A., El Gouri, M., Safi, Z., Jalgham, R. T. T., Wazzan, N., Verma, C., Ebenso, E. E., & Pramod Kumar, U. (2019). Anticorrosive properties of hexa (3-methoxy propan-1,2-diol) cyclotri-phosphazene compound for carbon steel in 3% NaCl medium: Gravimetric, electrochemical, DFT and Monte Carlo simulation studies. Heliyon, *5*(3), e01340. https://doi.org/10.1016/j.heliyon.2019.e01340

Dennington, T. K R., & Millam, J. (2010). GaussView, Version 5. Semichem Inc.

Destegül, A., Akbaş, H., Karadağ, A., Canımkurbey, B., Yerli, Y., Tekin, K. C., Malayoğlu, U., & Kılıç, Z. (2019). Synthesis and structural and thermal properties of cyclotriphosphazene-based ionic liquids: Tribological behavior and OFET application. Ionics, *25*(7), 3211–3222.

Elgazzar, E., Dere, A., Özen, F., Koran, K., Al-Sehemi, A. G., Al-Ghamdi, A. A., Orhan Görgülü, A., El-Tantawy, F., & Yakuphanoglu, F. (2017). Design and fabrication of dioxyphenylcoumarin substituted cyclotriphosphazene compounds photodiodes. *Physica B: Condensed Matter*, *515*, 8–17.

Elmas, G., Okumuş, A., Sevinç, P., Kılıç, Z., Açık, L., Atalan, M., Türk, M., Deniz, G., & Hökelek, T. (2017). Phosphorus–nitrogen compounds. Part 37. Syntheses and structural characterizations, biological activities of mono and bis(4-fluorobenzyl)spirocyclotetraphosphazenes. *New Journal of Chemistry*, *41*(13), 5818–5835.

Fei, S.-T., Lee, S.-H. A., Pursel, S. M., Basham, J., Hess, A., Grimes, C. A., Horn, M. W., Mallouk, T. E., & Allcock, H. R. (2011). Electrolyte infiltration in phosphazene-based dye-sensitized solar cells. *Journal of Power Sources*, *196*(11), 5223–5230.

Fei, S.-T., Wood, R. M., Lee, D. K., Stone, D. A., Chang, H.-L., & Allcock, H. R. (2008). Inorganic–organic hybrid polymers with pendent sulfonated cyclic phosphazene side groups as potential proton conductive materials for direct methanol fuel cells. *Journal of Membrane Science*, *320*(1-2), 206–214.

Fleming, I. (2010). *Molecular orbitals and organic chemical reactions*. John Wiley & Sons, Ltd.

Frisch, M. J., Trucks, G. W., Schlegel, H. B., Scuseria, G. E., Robb, M. A., Cheeseman, J. R., Scalmani, G., Barone, V., Mennucci, B., Petersson, G. A., Nakatsuji, H., Caricato, M., Li, X., Hratchian, H. P., Izmaylov, A. F., Bloino, J., Zheng, G., Sonnenberg, J. L., Hada, M., Ehara, M., … Fox, D. J. (2010). Gaussian 09, Revision C.01. Gaussian, Inc.

Gleria, M., & De Jaeger, R. (2004). *Phosphazenes: A Worldwide Insight*. Nova Science Publishers.

Görgülü, A. O., Koran, K., Özen, F., Tekin, S., & Sandal, S. (2015). Synthesis, structural characterization and anti-carcinogenic activity of new cyclotriphosphazenes containing dioxybiphenyl and chalcone groups. Journal *of Molecular Structure*, *1087*, 1–10.

Hadji, D., & Rahmouni, A. (2016). Molecular structure, linear and nonlinear optical properties of some cyclic phosphazenes: A theoretical investigation. *Journal of Molecular Structure*, *1106*, 343–351.

İbişoğlu, H., Erdemir, E., Atilla, D., Şahin Ün, Ş., Topçu, S., & Gül Şeker, M. (2020). Synthesis, characterization and antimicrobial properties of cyclotriphosphazenes bearing benzimidazolyl rings. *Inorganica Chimica Acta*, *509*, 119679.

Ingle, S. T. K V. N., & Upadhyay, U. G. (2005). Glucosylation of 4′-hydroxychalcones using glucosyl donor. *Indian Journal of Chemistry*, *44B*, 801–805.

Januszewski, R., Dutkiewicz, M., Orwat, B., Maciejewski, H., & Marciniec, B. (2018). A library of multisubstituted cyclotriphosphazenes–molecular scaffolds for hybrid materials. *New Journal of Chemistry*, *42*(19), 15552–15555.

Jeyasheela, S., & Subramanian, K. (2019). Effect of biphenyl conjugation on the photosensitive properties of liquid crystalline polymers. *Journal of Molecular Structure*, *1180*, 411–419.

Jiang, X., Yu, G.-W., Li, Z.-G., Chu, S.-P., & Wang, S.-P. (2015). Synthesis and characterisation of phosphazene derivatives containing dioxybiphenyl and 4-sulfanylquinazoline groups. *Journal of Chemical Research*, *39*(3), 162–165.

Keser, S., Keser, F., Kaygili, O., Tekin, S., Turkoglu, I., Demir, E., Turkoglu, S., Karatepe, M., Sandal, S., & Kirbag, S. (2017). Phytochemical compounds and biological activities of *Celtis tournefortii* fruits. *Analytical Chemistry Letters*, *7*(3), 344–355.

Koopmans, T. (1934). Über die Zuordnung von Wellenfunktionen und Eigenwerten zu den Einzelnen Elektronen Eines Atoms. Physica, *1*(1-6), 104–113.

Koran, K. (2019). Structural, chemical and electrical characterization of organocyclotriphosphazene derivatives and their graphene-based composites. *Journal of Molecular Structure*, *1179*, 224–232.

Koran, K., & Görgülü, A. O. (2018). Structural characterizations, thermal behavior, and electrical measurements of the amidosulfonic acid catalyzed thermal ring-opening polymerization of substituted cyclotriphosphazene in 1,2,4-trichlorobenzene solution. *Advances in Polymer Technology*, *37*(8), 3229–3239.

Koran, K., Özen, F., Biryan, F., & Görgülü, A. O. (2016). Synthesis, structural characterization and dielectric behavior of new oxime-cyclotriphosphazene derivatives. *Journal of Molecular Structure*, *1105*, 135–141.

Koran, K., Tekin, C., Biryan, F., Tekin, S., Sandal, S., & Gorgulu, A. (2017). Synthesis, structural and thermal characterizations, dielectric properties and in vitro cytotoxic activities of new 2,2,4,4-tetra(4′-oxy-substituted-chalcone)-6,6-diphenylcyclotriphosphazene derivatives. *Medicinal Chemistry Research*, *26*(5), 962–974.

Koran, K., Tekin, Ç., Çalışkan, E., Tekin, S., Sandal, S., & Görgülü, A. O. (2017). Synthesis, structural and thermal characterizations and in vitro cytotoxic activities of new cyclotriphosphazene derivatives. *Phosphorus Sulfur*, *192*(9), 1002–1011.

Kuan, J.-F., & Lin, K.-F. (2004). Synthesis of hexa-allylamino-cyclotriphosphazene as a reactive fire retardant for unsaturated polyesters. *Journal of Applied Polymer Science*, *91*(2), 697–702.

Lee, S. S., Mizar, P., Kucuk, O., & Ture, S. (2020). The reactions of cyclotriphosphazene with 2-(2-hydroxyethylamino)ethanol. Spectroscopic studies of the derived products. *Phosphorus, Sulfur, and Silicon and the Related Elements*, *195*(6), 454–410.

McBee, E. T., Okuhara, K., & Morton, C. J. (1965). Modified Friedel-crafts preparation of 2,2,4,4-tetrachloro-6,6-diphenylcyclotriphosphazatriene. *Inorganic Chemistry*, *4*(11), 1672–1673.

Mirzaei, S., Hadizadeh, F., Eisvand, F., Mosaffa, F., & Ghodsi, R. (2020). Synthesis, structure-activity relationship and molecular docking studies of novel quinoline-chalcone hybrids as potential anticancer agents and tubulin inhibitors. *Journal of Molecular Structure*, *1202*, 127310.

Morris, G. M., Huey, R., Lindstrom, W., Sanner, M. F., Belew, R. K., Goodsell, D. S., & Olson, A. J. (2009). AutoDock4 and AutoDockTools4: Automated docking with selective receptor flexibility. *Journal of Computational Chemistry*, *30*(16), 2785–2791.

Mosmann, T. R., Cherwinski, H., Bond, M. W., Giedlin, M. A., & Coffman, R. L. (1986). Two types of murine helper T cell clone. I. Definition according to profiles of lymphokine activities and secreted proteins. *Journal of Immunology*, *136*(7), 2348–2357.

Mulliken, R. S. (1934). A new electroaffinity scale; together with data on valence states and on valence ionization potentials and electron affinities. *The Journal of Chemical Physics*, *2*(11), 782–793.

Murphy, W. S., & Wattanasin, S. (1980). Intramolecular alkylation of phenols. Part 5. A regiospecific anionic ring closure of phenols via quinone methides. Journal of the Chemical Society, Perkin Transactions, 1, 1567–1577.

Nikovskii, I. A., Chistyakov, E. M., & Tupikov, A. S. (2018). Phosphazene-Containing Ligands and Complexes on Their Base. *Russian Journal of General Chemistry*, *88*(3), 474–494.

Özcan, E., Tümay, S. O., Keşan, G., Yeşilot, S., & Çoşut, B. (2019). The novel anthracene decorated dendrimeric cyclophosphazenes for highly selective sensing of 2,4,6-trinitrotoluene (TNT). *Spectrochimica Acta. Part A, Molecular and Biomolecular Spectroscopy*, *220*, 117115. https://doi.org/10.1016/j.saa.2019.05.020

Parr, R. G., & Pearson, R. G. (1983). Absolute hardness: Companion parameter to absolute electronegativity. *Journal of the American Chemical Society*, *105*(26), 7512–7516.

Parr, R. G., Szentpály, Lv., & Liu, S. (1999). Electrophilicity Index. *Journal of the American Chemical Society*, *121*(9), 1922–1924.

Pearson, R. G. (1985). Absolute electronegativity and absolute hardness of Lewis acids and bases. *Journal of the American Chemical Society*, *107*(24), 6801–6806.

Politzer, P., Laurence, P. R., & Jayasuriya, K. (1985). Molecular electrostatic potentials: An effective tool for the elucidation of biochemical phenomena. *Environmental Health Perspectives*, *61*, 191–202. https://doi.org/10.1289/ehp.8561191

Prota, A. E., Danel, F., Bachmann, F., Bargsten, K., Buey, R. M., Pohlmann, J., Reinelt, S., Lane, H., & Steinmetz, M. O. (2014). The novel microtubule-destabilizing drug BAL27862 binds to the colchicine site of tubulin with distinct effects on microtubule organization. *Journal of Molecular Biology*, *426*(8), 1848–1860. https://doi.org/10.1016/j.jmb.2014.02.005

Satyanarayana, M., Tiwari, P., Tripathi, B. K., Srivastava, A. K., & Pratap, R. (2004). Synthesis and antihyperglycemic activity of chalcone based aryloxypropanolamines. *Bioorganic & Medicinal Chemistry*, *12*(5), 883–889.

Sengupta, S., & Thomas, S. A. (2006). Drug target interaction of tubulin-binding drugs in cancer therapy. *Expert Review of Anticancer Therapy*, *6*(10), 1433–1447. https://doi.org/10.1586/14737140.6.10.1433

Shaw, R. A. (1986). The phosphazenes–structural parameters and their relationships to physical and chemical properties. *Phosphorus and Sulfur and the Related Elements*, *28*(1-2), 99–128.

Shenvi, S., Kumar, K., Hatti, K. S., Rijesh, K., Diwakar, L., & Reddy, G. C. (2013). Synthesis, anticancer and antioxidant activities of 2,4,5-trimethoxy chalcones and analogues from asaronaldehyde: structure-activity relationship. *European Journal of Medicinal Chemistry*, *62*, 435–442. https://doi.org/10.1016/j.ejmech.2013.01.018

Singh, N. K., & Singh, S. B. (2002). Biological and solid state electrical conductance properties of the complexes of 1-salicyloyl-4-benzoyl-3-thiosemicarbazide with manganese(II), cobalt(II), nickel(II), copper(II), and zinc(II). *Synthesis and Reactivity in Inorganic and Metal-Organic Chemistry*, *32*(1), 25–47.

Siwy, M., Sek, D., Kaczmarczyk, B., Jaroszewicz, I., Nasulewicz, A., Pelczyńska, M., Nevozhay, D., & Opolski, A. (2006). Synthesis and

in vitro antileukemic activity of some new 1,3-(oxytetraethylenoxy)cyclotriphosphazene derivatives. *Journal of Medicinal Chemistry*, *49*(2), 806–810. https://doi.org/10.1021/jm0490078

Tanrıverdi Eçik, E., Şenkuytu, E., Okutan, E., & Yenilmez Çiftçi, G. (2019). Synthesis of BODIPY-cyclotetraphosphazene triad systems and their sensing behaviors toward Co(II) and Cu(II). *Inorganica Chimica Acta*, *495*, 119009.

Trott, O., & Olson, A. J. (2010). AutoDock Vina: Improving the speed and accuracy of docking with a new scoring function, efficient optimization, and multithreading. *Journal of Computational Chemistry*, *31*(2), 455–461. https://doi.org/10.1002/jcc.21334

Tümer, Y., Asmafiliz, N., Zeyrek, C. T., Kılıç, Z., Açık, L., Çelik, S. P., Türk, M., Çağdaş Tunalı, B., Ünver, H., & Hökelek, T. (2018). Syntheses, spectroscopic and crystallographic characterizations of cis- and trans-dispirocyclic ferrocenylphosphazenes: Molecular dockings, cytotoxic and antimicrobial activities. *New Journal of Chemistry*, *42*(3), 1740–1756.

Wang, L., Yang, Y.-X., Shi, X., Mignani, S., Caminade, A.-M., & Majoral, J.-P. (2018). Cyclotriphosphazene core-based dendrimers for biomedical applications: An update on recent advances. *Journal of Materials Chemistry B*, *6*(6), 884–895. https://doi.org/10.1039/c7tb03081a

Xie, L., Zhai, X., Liu, C., Li, P., Li, Y., Guo, G., & Gong, P. (2011). Anti-tumor activity of new artemisinin–chalcone hybrids. *Archiv Der Pharmazie*, *344*(10), 639–647.

Yang, G., Wu, W.-H., Wang, Y.-H., Jiao, Y.-H., Lu, L.-Y., Qu, H.-Q., & Qin, X.-Y. (2019). Synthesis of a novel phosphazene-based flame retardant with active amine groups and its application in reducing the fire hazard of Epoxy Resin. *Journal of Hazardous Materials*, *366*, 78–87. https://doi.org/10.1016/j.jhazmat.2018.11.093

Yang, W., & Parr, R. G. (1985). Hardness, softness, and the Fukui function in the electronic theory of metals and catalysis. *Proceedings of the National Academy of Sciences of the United States of America*, *82*(20), 6723–6726. https://doi.org/10.1073/pnas.82.20.6723